

## INFORMATION TO USERS

The most advanced technology has been used to photograph and reproduce this manuscript from the microfilm master. UMI films the text directly from the original or copy submitted. Thus, some thesis and dissertation copies are in typewriter face, while others may be from any type of computer printer.

The quality of this reproduction is dependent upon the quality of the copy submitted. Broken or indistinct print, colored or poor quality illustrations and photographs, print bleedthrough, substandard margins, and improper alignment can adversely affect reproduction.

In the unlikely event that the author did not send UMI a complete manuscript and there are missing pages, these will be noted. Also, if unauthorized copyright material had to be removed, a note will indicate the deletion.

Oversize materials (e.g., maps, drawings, charts) are reproduced by sectioning the original, beginning at the upper left-hand corner and continuing from left to right in equal sections with small overlaps. Each original is also photographed in one exposure and is included in reduced form at the back of the book. These are also available as one exposure on a standard 35mm slide or as a 17" x 23" black and white photographic print for an additional charge.

Photographs included in the original manuscript have been reproduced xerographically in this copy. Higher quality 6" x 9" black and white photographic prints are available for any photographs or illustrations appearing in this copy for an additional charge. Contact UMI directly to order.

# U·M·I

University Microfilms International  
A Bell & Howell Information Company  
300 North Zeeb Road, Ann Arbor, MI 48106-1346 USA  
313 761 4700 800 521 0600

Order Number 1336844

**Modeling of viscosities in liquid melts and experimental  
determination of spent potlining**

Hu, Huijun, M.S.

University of Nevada, Reno, 1989

**U·M·I**  
300 N. Zeeb Rd.  
Ann Arbor, MI 48106

University of Nevada

Reno

MODELING OF VISCOSITIES IN LIQUID MELTS AND  
EXPERIMENTAL DETERMINATION OF SPENT POTLINING

A thesis submitted in partial fulfillment of the  
Requirements for the degree of Master of Science in  
Metallurgical Engineering

By

Huijun Hu

1989

The thesis of Hu is approved:

*Ramona Reddy*

---

Thesis Advisor

*John W. Smith*

---

Department Chair

*Ann Fenn*

---

Dean, Graduate School

University of Nevada

Reno

FEBRUARY 1989

## ACKNOWLEDGEMENT

I wish to express my many thanks to Dr.R.G.Reddy, all the work presented here had been done under his helpful guidance. Thanks are also due to Dr.D.Chandra and Dr.L.C.Hsu for their interest in this research.

I express my sincere thanks to Mr.R.Lee.Byers and Mr.H.J.Hitther, ALCOA fondation, Grant # 20585, Pittsburgh, PA, for their support this research.

This research was supported by the Department of the Interior's Mineral Institutes program administered by the Bureau of Mines under allotment grant Number G1154132. I sincerly express my appreciation to Mackay Minerals Resources Research Institute and also to the program development funds, University of Nevada-Reno for the financial support during my studying in UNR.

## ABSTRACT

The method of calculation of viscosity presented in this paper lead to reasonably accurate values in the composition range of  $0.3 < X_{SiO_2} < 1$ , for binary, ternary and multicomponent systems. The  $NO^{\circ}$ ,  $NO^{-}$  and  $NO^{2-}$  ions distribution in the melts has been evaluated based on the depolymerization reaction. The  $NO^{\circ}$  values obtained by the atomic pair model agrees very well with the experimental data. An equation was derived using the hole theory to express the temperature and  $NO^{\circ}$  dependence of viscosity. The deduced equation

$$\eta = 4.9 \times 10^{-9} T^{1/2} NO^{\circ} \exp(E/RT) \quad (\text{poise})$$

is successfully applied to predict the viscosity of several binary, ternary and multicomponent systems. Excellent agreement between calculated viscosity values and experimental data for several temperature was observed.

Viscosities of industrial spent potlining(SPL) were measured as a function of temperature and with the oxide addition to the SPL. The results showed that the viscosity of SPL decreased with increasing temperature and also decreased with the addition of 20 wt% CaO and 20 wt% SiO<sub>2</sub> to SPL.

TABLE OF CONTENTS

|  | Page    |
|--|---------|
| LIST OF TABLES   | v i     |
| LIST OF FIGURES  | v i i i |
| MODELING OF VISCOSITIES IN LIQUID MELTS AND<br>EXPERIMENTAL DETERMINATION OF SPENT POTLINING | 1       |
| 1. CHAPTER   | 2       |
| 1.1 INTRODUCTION   | 2       |
| 1.2 PREVIOUS WORK  | 3       |
| 1.3 PRESENT WORK   | 7       |
| 2. CHAPTER   | 8       |
| 2.1 THEORETICAL CONSIDERATIONS   | 8       |
| 2.1.1 KINETICAL THEORY CONSIDERATIONS  | 8       |
| 2.1.2 STRUCTURE THEORY CONSIDERATIONS  | 13      |
| 2.2 EVALUATION OF A MODEL  | 25      |
| 3. CHAPTER   |         |
| CALCULATION AND DISCUSSION   | 28      |
| 3.1 PURE LIQUID SILICA   | 28      |
| 3.2 BINARY SYSTEMS   | 28      |
| 3.2.1 ALKALI METAL OXIDE-SILICA SYSTEMS  | 28      |
| 3.2.2 ALKALINE EARTH METAL OXIDE-SILICA<br>SYSTEMS   | 30      |
| 3.2.3 ALUMINUM-SILICA SYSTEM   | 36      |

## TABLE OF CONTENTS (CONTINUED)

|                            |     |    |
|----------------------------|-----|----|
| 3.3 TERNARY SYSTEMS        | --- | 45 |
| 3.4 MULTICOMPONENT SYSTEMS | --- | 51 |
| 4. CHAPTER                 | --- | 54 |
| 4.1 INTRODUCTION           | --- | 54 |
| 4.2 EXPERIMENTS            | --- | 55 |
| 4.3 RESULTS AND DISCUSSION | --- | 58 |
| 5. CHAPTER                 |     |    |
| CONCLUSION                 | --- | 62 |
| 6. CHAPTER                 |     |    |
| REFERENCES                 | --- | 63 |



## LIST OF TABLES

|   | Page   |
|---|--------|
| Table 1. Free energy of formation compounds   | --- 29 |
| Table 2. Calculated and measured viscosity of<br>alkali metal-silicate binary systems.            | --- 31 |
| Table 3. Calculated and measured viscosity of alkali<br>earth metal-silicate systems. (at 1973K)  | --- 37 |
| Table 4. Calculated and measured viscosity of alkali<br>earth metal-silicate systems. (at 2023 K) | --- 38 |
| Table 5. Calculated and measured viscosity of alkali<br>earth metal-silicate systems. (at 2073 K) | --- 39 |
| Table 6. Calculated and measured viscosity of<br>alumina-silicate system. (2223 K)                | --- 44 |
| Table 7. Calculated and measured viscosity of<br>MnO-CaO-SiO <sub>2</sub> system. (1773 K).       | --- 48 |
| Table 3. Calculated and measured viscosity of<br>MgO-CaO-SiO <sub>2</sub> system. (1623 K).       | --- 48 |

|   |     |    |
|---|-----|----|
| Table 9. Calculated and measured viscosity of<br>CaO-SiO <sub>2</sub> -Al <sub>2</sub> O <sub>3</sub> system. (1773 K)      | --- | 50 |
| Table 10. Calculated and measured viscosity of<br>SrO-SiO <sub>2</sub> -Al <sub>2</sub> O <sub>3</sub> system (1843 K).     | --- | 50 |
| Table 11. Calculated and measured viscosity of<br>CaO-MgO-SiO <sub>2</sub> -Al <sub>2</sub> O <sub>3</sub> system (1773 K). | --- | 53 |
| Table 14. The chemical composition of SPL   | --- | 56 |

## LIST OF FIGURES

|  | Page   |
|--|--------|
| Fig.1. Viscous forces arise from transfer of momentum between adjacent layers in fluid.                              | --- 9  |
| Fig.2. Different Si-O group distribution in polymerization melts(CaO-SiO <sub>2</sub> binary system).                | --- 14 |
| Fig.3. The three type oxygen anions distribution in PbO-SiO <sub>2</sub> system at 1673 K.                           | --- 19 |
| Fig.4 Plot of calculated and measured NO <sup>o</sup> in binary system.  | --- 20 |
| Fig.5. Schematic diagram to show a segment of an SiO <sub>4</sub> chain breaking off and jumping into an empty hole. | --- 21 |
| Fig.6 Activation energy changes in binary systems.   | --- 23 |
| Fig.7. 1. The mass balance for depolymerization  | --- 26 |
| 2.The structure of tetrahedra and triangle.  | --- 26 |
| Fig.8. Plot of calculated and measured viscosity of binary systems at 1623 K.  | --- 32 |
| Fig.9. Plot of calculated and measured viscosity of binary systems at 1673 K.  | --- 33 |
| Fig.10. Plot of calculated and measured viscosity of binary systems at 1723 K.                                       | --- 34 |

|   |     |    |
|---|-----|----|
| Fig.11. Plot of calculated and measured viscosity of binary systems as a function of temperature. | --- | 35 |
| Fig.12. Plot of calculated and measured viscosity of binary systems at 1973 K.                    | --- | 40 |
| Fig.13. Plot of calculated and measured viscosity of binary systems at 2023 K.                    | --- | 41 |
| Fig.14. Plot of calculated and measured viscosity of binary systems at 2073 K.                    | --- | 42 |
| Fig.15. Plot of calculated and measured viscosity of ternary system at 1773 K.                    | --- | 49 |
| Fig.16. The experimental set-up.  | --- | 57 |
| Fig.17. The measured viscosities data of SPL.   | --- | 59 |

\*\*\*\*\*  
\*  
\*  
\*       MODELING OF VISCOSITIES IN LIQUID MELTS AND       \*  
\*       EXPERIENTAL DETERMINATION OF SPENT POTLINING       \*  
\*  
\*  
\*\*\*\*\*

## 1. CHAPTER

### 1.1. INTRODUCTION

Molten slags, which are mainly oxide mixture, play an important role in many metallurgical processes. For this reason, there has been an interest in the molten silicate slags. Viscosity of molten slags is one of most important properties. This is because the kinetic processes in slag-metal, slag-gas, and the slag-gas-metal systems are often controlled by mass diffusion in the boundary layer of the slag phase. As a consequence, the factors determining the boundary layer thickness of the slag phase where the transport processes occur are also important. This is related to the viscosity of the slag phase. It has been known that if the slags are too fluid, non-uniform liquid layer may form; if the slags are too viscous, a discontinuous film may result. Either of these conditions is not acceptable in metallurgical casting processes.

The viscosity of silicate melts and slags is a property difficult to experimentally measure accurately. It is both time consuming and expensive. The use of models to estimate the viscosity is the first step to be carried out, mainly with metallurgical slags involving numerous components. A great deal of research work on viscosity have been done(1-3). The purpose of this work is to present a simple relation directly related to viscosity which can be applied to all the systems.

## 1.2. PREVIOUS WORK

Viscosity is strongly dependent on the temperature and composition of the liquid. The typical relationship between viscosity-temperature was proposed by Andrade-Arrhenius where the log of viscosity is a linear function of the reciprocal absolute temperature. Since then, a variety of models have been developed. Glasstone, Laidler and Eyring(5) proposed an absolute rate theory, a theoretical extension of the Andrade-Arrhenius equation. In this model, viscous flow can be viewed as a rate process dominated by transition state of high energy. Transport over the energy barriers is biased by the applied stress, and the standard treatment yields an expression for the viscosity

$$\eta = \frac{\exp(\Delta E/kT)}{2 \tau \sinh(V/2kT)} \quad (1-1)$$

where  $\tau$  is the shear stress,  $\Delta E$  is the height of the energy barrier in the absence of stress,  $\nu$  is the number of times per second the barrier is attempted, and  $V$  is the flow volume. For small stress, the viscosity on this model should be independent of stress; at large stresses, the viscosity should decrease strongly with increasing temperature. For the small-stress case, appropriate in most experimental situations, Eq (1-1) becomes

$$\eta = \frac{kT}{V} \exp\left(-\frac{E}{kT}\right) \quad (1-2)$$

This expression is similar to Arrhenius equation.

A equation which contains a free volume term has been developed by Turnbull and Cohen(5). According to this model, the critical step in flow is opening a void of some critical volume to permit molecular motion. The void is viewed as being formed by the redistribution of the free volume  $V_f$  in the system. The free volume is defined as:

$$V_f = V_m - V_o \quad (1-3)$$

where  $V_m$  is the molecular volume at a given temperature and  $V_o$  is the effective hard-core volume of the molecule. Under most conditions where flow is observed, the average free volume is a small fraction of the viscosity.

$$\eta = B \exp\left(-\frac{KV_o}{V_f}\right) \quad (1-4)$$

where B and K are constants. The temperature dependence of the viscosity is represented here by the temperature dependence of the free volume. By assuming that  $V_f$  falls to some small value in the vicinity of the glass transition  $T_g$ ,



the familiar Williams-Landel Ferry (WLF) relation is obtained. Applied to viscosity, this relation is

$$\eta = B \exp[b/(f_g + (T-T_g))] \quad (1-5)$$

Here,  $f_g$  is the fraction of free volume at the glass transition.

Adam and Gibbs(6) considered a model for viscosity which can be expressed as:

$$\eta = C \exp ( D/TS_c ) \quad (1-6)$$

Where  $C$  is a constant,  $S_c$  is the configurational entropy of the component in the melt, and  $D$  is nearly constant, proportional to the potential-energy barrier to molecular rearrangement. Over a range of temperature near  $T_g$ , this expression is effectively indistinguishable from the WLF relation. but, both of these can be expressed as:

$$\eta = E \exp [F/(T-T_o)] \quad (1-7)$$

where  $E$  and  $F$  are constants.

In an attempt to simplify the representation of the composition dependence of the viscosity of complex systems, several empirical correlations have been developed. Turkdogan and Bills(7) showed that the viscosity of

CaO-Al<sub>2</sub>O<sub>3</sub>-SiO<sub>2</sub> melts as a function of composition could be represented in a simple manner by using a silica equivalence for the concentration of alumina. The correlation obtained by Higgins and Jones(8) is based on the ion-oxygen interaction parameter. Toguri et al(9) showed that for copper smelting slags the viscosity isotherm may be plotted simply against the slag basicity. Bottinga and Weill(10) developed an empirical method of estimating the viscosity of complex aluminosilicates with emphasis on the silicate liquids. The formulation is based on the Arrhenius mixture rule. Recently, Urbain(11) proposed a correlation between viscosity and temperature, which has the form  $\eta = A \exp(B/T)$ . The parameters A and B in the above equation were correlated to the composition of the melts used.

### 1.3 PRESENT WORK

The present study included three aspects:

1. A viscosity model as a function of temperature, compositions of the melts was developed using the concepts of hole theory and atomic pair model. The calculated viscosity values for Alkali metal and Alkali earth metal oxide-silica systems are in good agreement with the experimental data.
2. The model has been extended to apply to multicomponents systems. The predicted viscosity values appear to be in excellent agreement with the experimental data.
3. The viscosity of industrial spent potlining were measured as a function of temperature and addition of 20 wt% CaO or SiO<sub>2</sub> to the SPL. The results show that the viscosities of SPL decreased with increasing temperature and also decreased with the addition of CaO and SiO<sub>2</sub>.

## 2. CHAPTER

### 2.1. THEORETICAL CONSIDERATIONS

#### 2.1.1 KINETICAL THEORY CONSIDERATIONS

Viscosity is defined as the ratio of shear stress and velocity gradient:

$$\tau = \eta \frac{dV_x}{dy} \quad (2-1)$$

The unit of viscosity is the poise (P), in SI units,  $0.1 \text{ N s m}^{-2}$ , and in CGS units,  $1 \text{ dyn s cm}^{-2}$ .

The viscous momentum flux, as shown in Fig.1, is in the direction of the negative velocity gradient. Viscous flow is a momentum transport process in the fluid phase. Based on this view, Bokrice and Reddy(12) derived a viscosity expression using kinetic theory principles.

Consider three parallel layers of fluid, A, B, and C (Fig.1), moving with velocities  $V + (\partial V / \partial z)L$ ,  $V$ , and  $V - (\partial V / \partial z)L$ , respectively, where  $z$  is the direction normal to the planes and  $L$  is the mean free path of the particles populating the layers, i.e., the mean distance traveled by the particles without undergoing collisions. In the direction of motion of the moving layers, the moments of the particles traveling in the A, B and C layers is  $m[V + (\partial V / \partial z)L]$ ,  $mV$ , and  $m[V - (\partial V / \partial z)L]$ , respectively.

When a particle jumps from the A to B layer, the momentum gained by the B layer is  $-m(\partial V / \partial z)L$ , i.e., the momentum

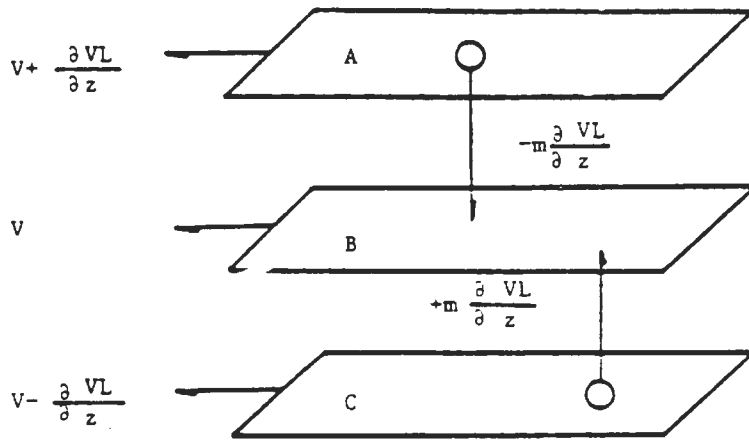


Fig.1 Viscous forces arise from transfer of momentum between adjacent layers in fluid

transported per particle in the downward direction is  $-m(\partial V/\partial z)L$ . If one considers that there are  $N$  particles per unit area,  $B$  layer is  $A \text{ cm}^2$  and  $W$  is the mean velocity of particles in the direction normal to the layers, the momentum transferred per second in the downward direction owing to  $A - B$  jumps is  $-[NWA m(\partial V/\partial z)L]$ . This rate of change of momentum is equal to a force (Newton's second law of motion). Thus, the viscous force  $F$  is given by

$$F = -(2NWA m) A \partial V/\partial z \quad (2-2)$$

But, according to Newton's law of viscosity, the viscous force is proportional to the area of the layers and to the velocity gradient, and the proportionality constant is the viscosity, i.e.,

$$F = -\eta A \partial V/\partial z \quad (2-3)$$

Combining Eq.(2-2) and (2-3), it is clear that

$$\eta = 2 N m W \quad (2-4)$$

For the fused slags, the hole model has been proposed by Furth(13). It is considered that the sizes and spatial location of the empty regions in the fused slags are random. These randomly located and variable-sized vacancies are

called holes. Holes move at finite velocities and have an inertial resistance to motion, i.e., have masses and momenta. According to the hole theory, holes play the role in pure ionic liquids. Thus, it is considered that the random walk of holes between adjacent layers results in momentum transfer and, therefore, viscous drag in a moving fused slags exists. The expression for the viscosity of an ionic liquid, on the basis of this model, is

$$\eta = 2 N_h m_h W \quad (2-5)$$

where  $N_h$  and  $m_h$  are the number of holes per unit volume and the mass of holes, respectively. Eq.(2-5) shows a very simple expression for viscosity. To enable us to estimate viscosity of liquid systems, it is necessary to express the above terms for liquid melts.

Now, the velocity component  $W_h$  is given by the ratio of the mean time between collisions.

$$W_h = L / \tau \quad (2-6)$$

the viscosity can be written as follows

$$\eta = 2 N_h \tau [m_h (W_h)^2] \quad (2-7)$$

The theorem of the equipartition of energy can now be applied to the one dimensional motion referred to  $W_h$

$$\frac{1}{2} m_h (W_h)^2 = \frac{1}{2} K T \quad (2-8)$$

Substituting Eq.(2-8) into Eq.(2-7), one obtains:

$$\eta = 2 N_h K T t \quad (2-9)$$

In a fused slags,  $t$  is the mean lifetime of a hole, i.e., the average time between creation and destruction of a hole through thermal fluctuations. It is given by(12):

$$t = (R_h/3) (6.28 m / K T)^{1/2} \exp(E/RT) \quad (2-10)$$

where  $R_h$  is the average radius of the hole,  $m$  is the mass of particle and  $E$  is the activation energy of particle to overcome the barrier to move to an adjacent hole. Combining Eq.(2-9) and (2-10), the equation (2-11) can be obtained as:

$$\eta = (2/3) N_h R_h (6.28 m K T)^{1/2} \exp(E/RT) \quad (2-11)$$

This is a kinetic model to calculate viscosity. The quantities in Eq.(2-11), such as activation energy  $E$ , the number of holes  $N_h$  and the radii of hole  $R_h$ , need to be determined and are discussed in the next section.



### 2.1.2. STRUCTURE THEORY CONSIDERATIONS

Thermodynamic properties of silicate melts have been studied for a long time, but a description of the structure of liquid silicate has been attempted only over the last few decades. With the development of modern techniques, X-ray diffraction and scanning electron microscope are used to study the structure of silica melts. These studies have provided more information about the structure of silicate and made it possible to understand the structure of liquid silicates.

Liquid silicates are much more complex than solid ones, because their constituents may have different types of Si-O group(14). With the assumption of equilibrium of polyanions entities in the liquid at each temperature and composition, Si can form  $\text{SiO}_4$  ( $\text{SiO}_4$  is used instead  $\text{SiO}_4^{-4}$  for convenience in following),  $\text{Si}_2\text{O}_7$  and  $\text{Si}_n\text{O}_{3n+1}$ . Therefore, there is a wide distribution of anions of different sizes in the polymeric melts as shown in Fig.2. It has been shown that the basic building unit is  $\text{SiO}_4$  tetrahedra(15) which share corners with one another in silicate melts. The addition of metal oxides to silicate melt causes depolymerization resulting in a breakdown of the silicate network structure. The depolymerization reaction can be written as



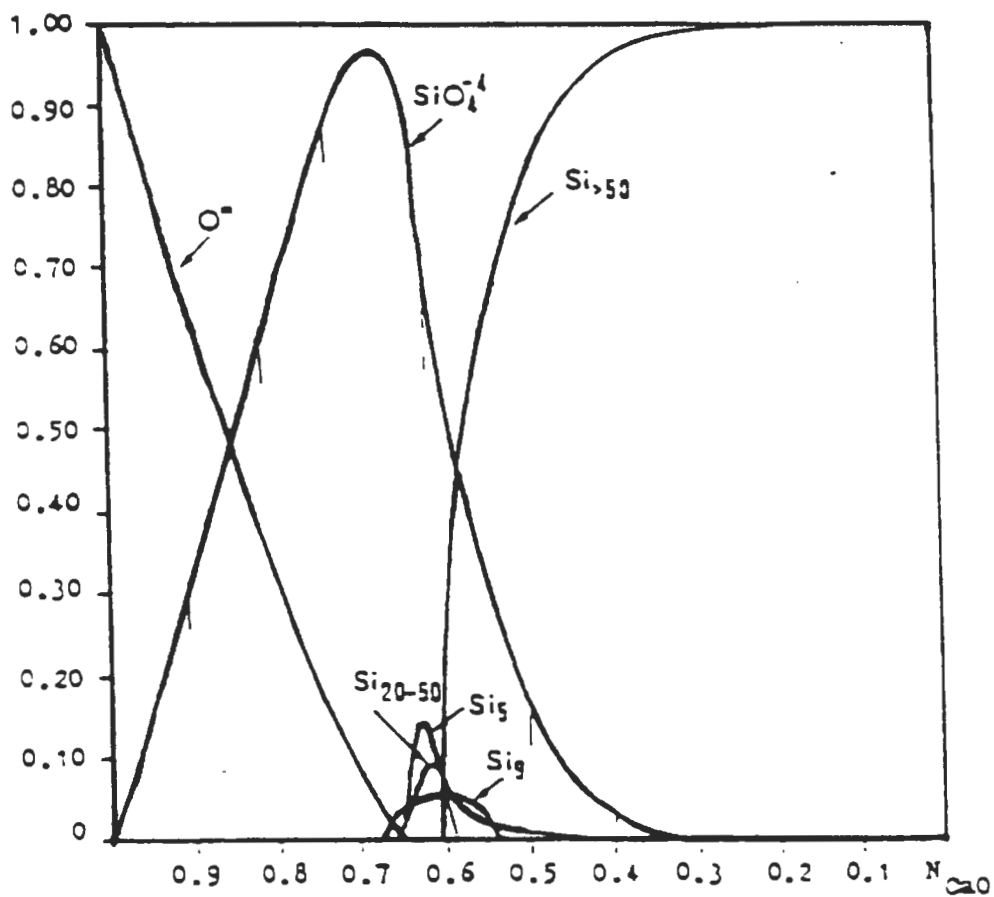


Fig.2 Different Si-O group distribution in polymerization melts. (CaO-SiO<sub>2</sub>)

expressing in terms of a simple electrochemical reaction:



where  $O^{\circ}$  is a bridging oxygen bonded to two silicon atoms;  $O^{-}$  is an oxygen bonded to only one silicon atom and  $O^{2-}$  is free oxygen ion. In general, the more  $O^{\circ}$  ions concentration in the silicate melts, the greater the extent of polymerization. Using statistical thermodynamic methods, the distribution of ionic fractions of  $NO^{\circ}$ ,  $NO^{-}$  and  $NO^{2-}$  was computed and is discussed below.

A. The ions distribution in  $SiO_2$  system:

Let N moles of  $SiO_2$  and M moles of basic oxide, MO, react to form a binary silicate melt, the liquid melt is considered as a mixture of cation( $M^{++}$ ) and anions( $O^{\circ}$ ,  $O^{-}$  and  $O^{2-}$ ). The charge and mass balance considerations, respectively, require that(see Fig.7-1)

$$NO^{\circ} = 2N - 1/2 NO^{-} \quad (2-14)$$

$$NO^{2-} = M - 1/2 NO^{-} \quad (2-15)$$

the total number of anions

$$NO^{\circ} + NO^{2-} + NO^{-} = 2N + M. \quad (2-16)$$

According to statistical theory, the number of ways of configuration of these pairs is given by

$$t_{\text{gen}} = N_{\text{total}}! / (NO^0)! (NO^-/2)! (NO^-/2)! (NO^{2-})! \quad (2-17)$$

substituting Eq.(2-14), Eq.(2-15) and Eq(2-16) to Eq.(2-17), Eq.(2-18) can be obtained as:

$$t_{\text{gen}} = \frac{(2N + M)!}{[1/2(2M-NO^-)]! (NO^-/2)! (NO^-/2)! [1/2(4N-NO^-)]!} \quad (2-18)$$

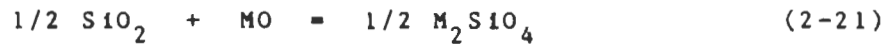
The normalized number of ways of configuration(16) is

$$\Omega' = \frac{[1/2(2-NO')]! (NO'/2)! (NO'/2)! [1/2(4N-NO')]! (N+M/2)!}{[1/2(2M-NO^-)]! (NO^-/2)! (NO^-/2)! [1/2(4N-NO^-)]! N!(1/2M)!} \quad (2-19)$$

where  $NO'$  is the value of  $NO^-$  at random mixing,  $NO' = 2NM/(N+2M)$ . The additional factor of the partition function of solution relative to the pure component melts can be expressed as

$$\Omega = \Omega' \exp(\Delta G^0/RT) \quad (2-20)$$

where  $\Delta G^0$  is free energy for reaction



The value of  $\text{NO}^-$  is determined by the condition that becomes maximum. Thus

$$\frac{\partial \ln \Omega}{\partial \text{NO}^-} = \ln \frac{[1/4(2\text{M}-\text{NO}^-)(4\text{N}-\text{NO}^-)]^{1/2}}{\text{NO}^-/2} - \frac{\Delta G^\circ}{\text{RT}} = 0 \quad (2-22)$$

let  $\text{M}+\text{N}=1$ , then  $\text{M} = X_{\text{MO}}$

Eq. (2-21) leads to

$$(2X_{\text{MO}} - \text{NO}^-)(4 - 4X_{\text{MO}} - \text{NO}^-) = \exp(\Delta G^\circ/\text{RT}) \text{NO}^{-2} \quad (2-22)$$

Thus, the  $\text{NO}^-$  values can be calculated by

$$(1 - \exp(\Delta G^\circ/\text{RT}))(\text{NO}^-)^2 + (2X_{\text{MO}} - 4)(\text{NO}^-) + 8X_{\text{MO}}(1 - X_{\text{MO}}) = 0 \quad (2-23)$$

The  $\text{NO}^\circ$  values can be derived by the definition:

$$\begin{aligned} \text{NO}^\circ &= 1/2(4\text{M} - \text{NO}^-)/(2\text{M} + \text{N}) \\ &= (4 - 4X_{\text{MO}} - \text{NO}^-)/2(2 - X_{\text{MO}}) \end{aligned} \quad (2-24)$$

The distribution of the three type oxygen ions,  $O^0$ ,  $O^-$  and  $O^{2-}$  in  $PbO-SiO_2$  binary system calculated using Eq.(2-23) and (2-24) is shown in Fig.3. As seen from Fig.3, the ions distribution can be divided into three regions. For  $X_{SiO_2} < 0.33$ , the complete depolymerization region is obtained, where only  $O^-$  and  $O^{2-}$  ions exist. For  $0.67 < X_{SiO_2} < 0.33$ , the partial depolymerization region is observed, where three types of oxygen ions exist and for  $X_{SiO_2} > 0.67$ , the complete polymerization region is observed, where no free oxygen ions exist.

The calculated  $NO^0$  values using equation(2-23) and (2-24) for  $PbO-SiO_2$  melts at 1673K are presented in Fig.4. Yasuari(17) experimentally determined the distribution of  $NO^0$ ,  $NO^-$  and  $NO^{2-}$  ions in the  $PbO-SiO_2$  melts using X-ray photoelectron method at 1673K. These data are also presented in Fig.4. As seen from the figure, an excellent agreement is obtained between the calculated and the experimental data.

#### B.The theoretical calculation of activation energy:

The hole theory shows(12) that the activation energy for a particle motion includes two steps. One is the energy required to form a hole( $E_1$ ) and another is the energy required to make a particle jump into the hole( $E_2$ ). For Si-O-Si network structure, hole are easily formed (the activation energy to form a hole equal,  $E_1=3.3 RT_m$  (12)), but it is difficulty to produce the jumping particles because

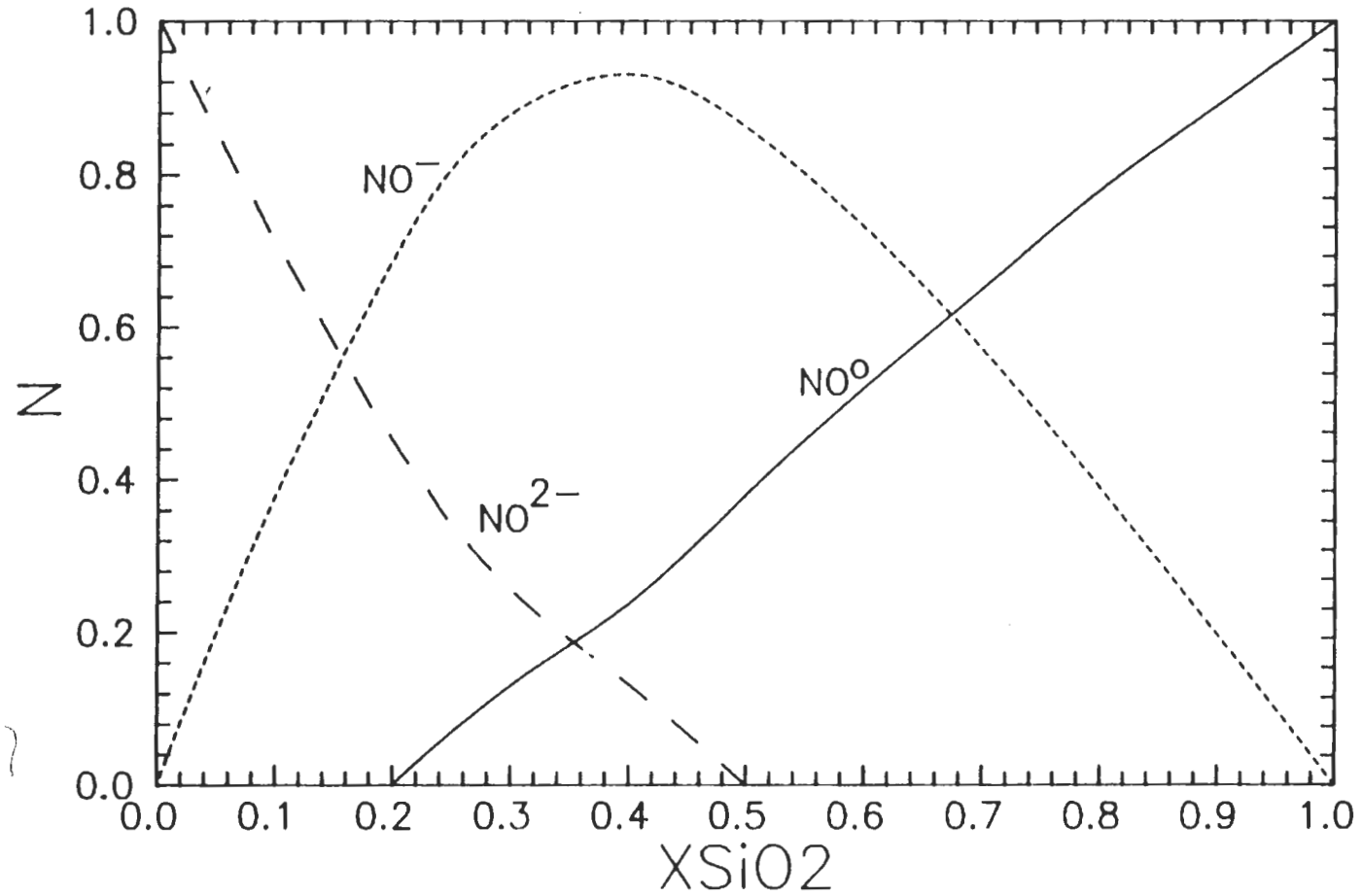


Fig.3 The three type oxygen anions distribution in PbO-SiO<sub>2</sub> system at 1673 K

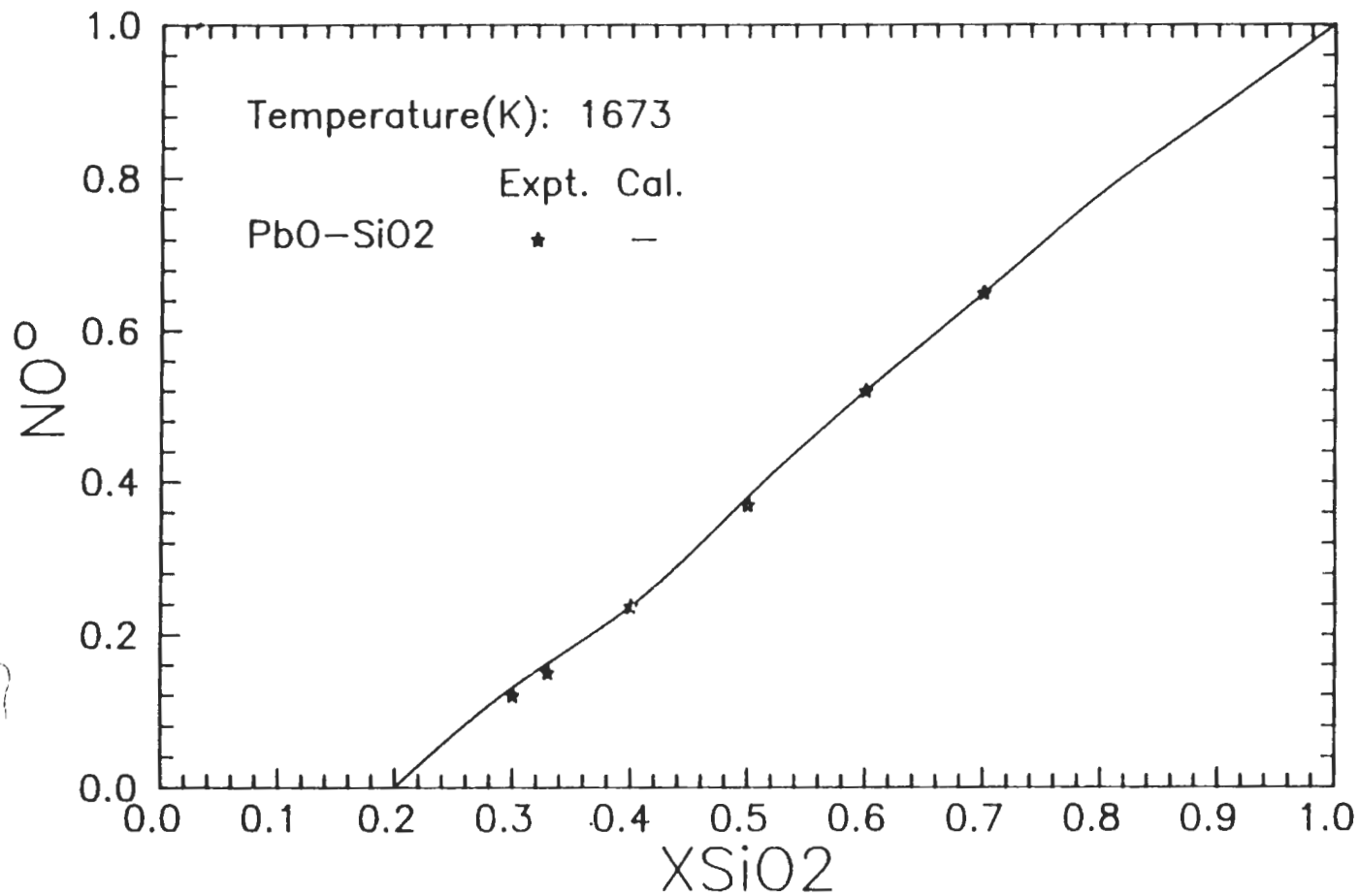


Fig 4. Plot of calculated and measured NO<sup>o</sup> in Binary system



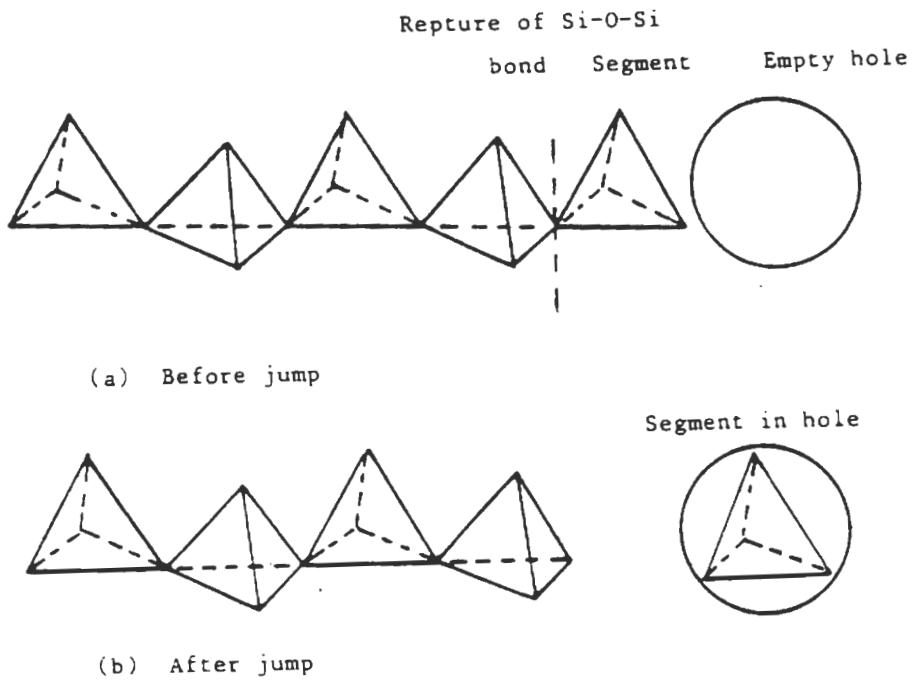


Fig.5 Schematic diagram to show a segment of a SiO<sub>2</sub> chain breaking off and jumping into an empty hole.

the Si-O bonds must be broken before it can jump as shown Fig.5. Thus, in associated liquids with network structures, the activation energy is determined by the energy required to break the bonds of the network. Obviously, the more the number of Si-O bonds (i.e.  $\text{NO}^\circ$  concentration), the more activation energy is needed.

The quantitative expressions as described above for the the calculation of  $\text{NO}^\circ$  in melts makes it possible to derive a mathematical relation between E and  $\text{NO}^\circ$ . It has been known that the activation energy E increased with increasing number of  $\text{NO}^\circ$ . The change of E with the degree of depolymerization is shown in Fig.6(18). As seen from the figure, E shows three distinct regions. The E decreases rapidly as metal oxide is added to  $\text{SiO}_2$  until about 20 mole% is dissolved in the melt, followed by a plateau that extends to about 50 mole% metal oxide additions. An additional increase in the metal oxide addition results in further decrease in the activation energy.

According to the curve showed in Fig.6, a mathematic expression between E and  $\text{NO}^\circ$  can be obtained. The rate of change of E with respect to  $\text{NO}^\circ$  could be expressed:

$$dE / d\text{NO}^\circ = A E^n \quad (2-25)$$

where A is constant and n is the power number. Equation

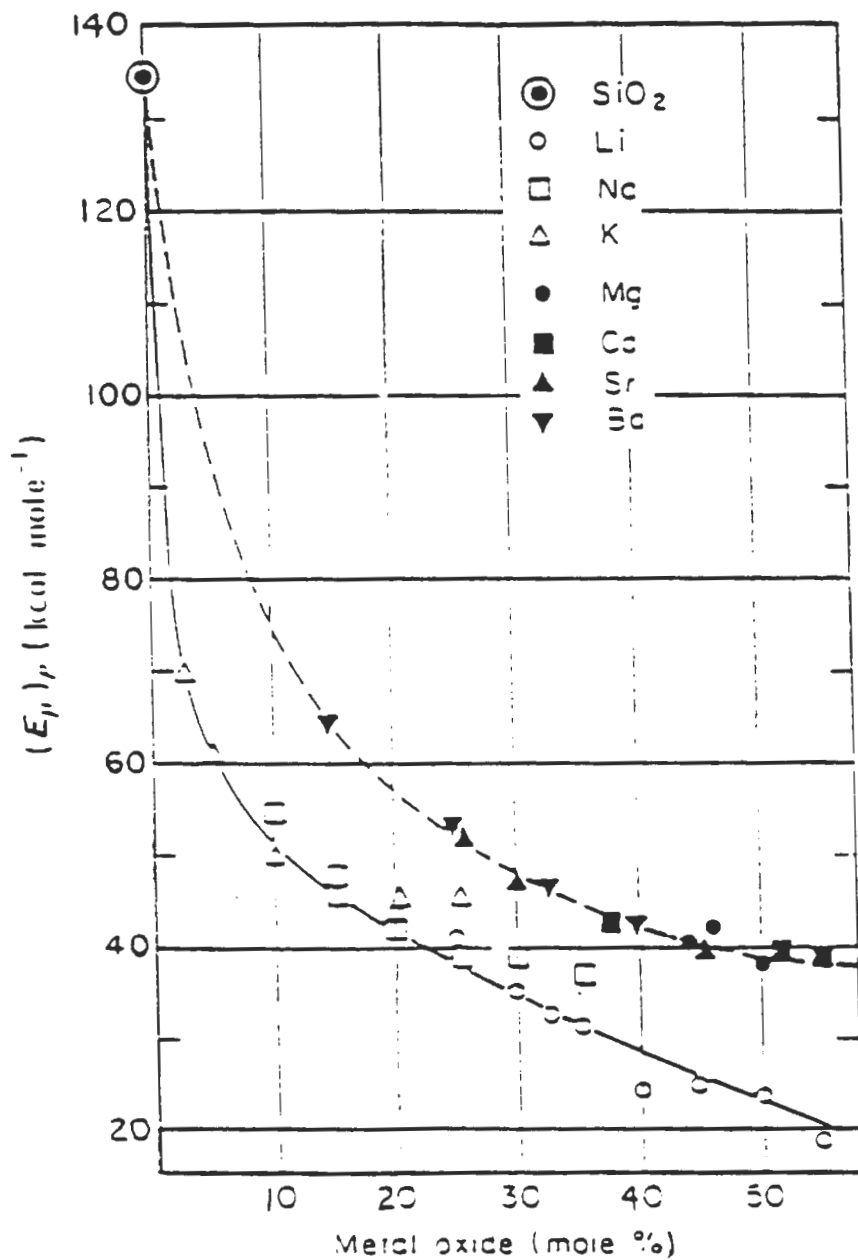


Fig.6 Activation energy changes in binary systems.

(2-25) was integrated for the known conditions of E and  $NO^0$ . For pure liquid silicate,  $NO^0=1$  and  $E^*=519$  kjoule/mole(19), for any other composition in binary melt,  $NO^0=NO^0$  and  $E = E$ . After intergration of equation (2-25), the expression obtained is

$$E = E^* / [AE^{*(n-1)} (n-1)(1-NO^0) + 1]^{1/(n-1)} \quad (2-26)$$

Let  $(n-1)=M$ ,  $K=AE^{*(n-1)}(n-1)$ , equation (2-27) can be rewritten as:

$$E = E^* / [K (1-NO^0) + 1]^{1/M} \quad (2-27)$$

The experimental data has been shown that the activation energy E will change with the type of cations. In general, the E in double charged cations cases is larger than that in single charged cations.

## 2.2. EVALUATION OF A MODEL

As discussed above, the expression of viscosity for silicate melts has been obtained:

$$\eta = 2/3 N_h R_h (6.28 \pi K T)^{1/2} \exp(E/RT) \quad (2-11)$$

and  $E$  as a function of  $NO^0$  was also derived and shown in equation (2-27).

The numerical values for  $R_h$ ,  $N_h$  and the term  $(6.28\pi K T)$  for silicate melts can be determined and are discussed below.

### 2.2.1. Determination of $R_h$

Furth(13) has showed that for a typical hole in a liquid, the size of a hole is roughly as same as an ion and can accommodate an ion. For  $SiO_4$  tetrahedra, the minimum radii of hole should be equal to the radii of  $SiO_4$  tetrahedra. The ionic radius of oxygen is 1.38 Å and the radius of silicon is 0.26 Å. According to this structure (see Fig.7-2), the radius of  $SiO_4$  tetrahedra can be deduced as 3.4 Å.

### 2.2.2. Determination of the term $(6.28\pi K T)^{1/2}$

This term can be rearranged as:

$$\begin{aligned} (6.28 \pi K T)^{1/2} &= (6.28 \pi / K T)^{1/2} K T \\ &= (6.28 \pi A_v / A_v K T)^{1/2} K T \\ &= (6.28 W / R T)^{1/2} K T \quad (2-28) \end{aligned}$$

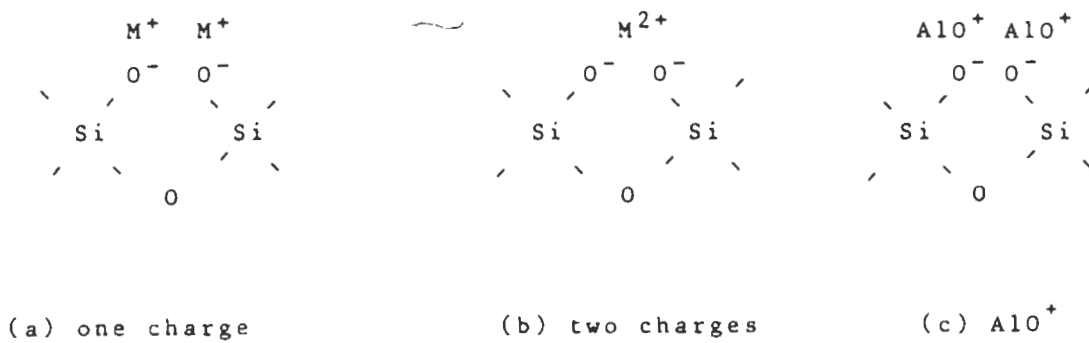


Fig.7-1 The mass balance for depolymerization



Fig.7-2 The structure of tetrahedra

Where  $K$  is Boltzmann constant ( $1.3 \times 10^{-23}$  Joules/degree),  $R$  is gas constant (8.3144 Joules/degree mole) and  $W$  is mole weight of the  $SiO_4$  tetrahedral unit, i.e.,  $W_{SiO_4} = 0.092$  kg/mole, Substituting  $R$ ,  $W$  and  $K$  into Eq.(2-30), We can obtain Eq.(2-29)

$$(6.28mKT)^{1/2} = 0.3637 \times 10^{-23} T^{1/2} \quad (2-29)$$

### 2.2.3. Determination of $N_h$

As mentioned above, the Si-O bonds must be broken before the  $SiO_4$  tetrahedral unit can jump into the hole. The assumptions are that the number of holes in the melt are equal to the number of tetrahedral units present in the melts and also that all the holes are filled by the tetrahedral units. Therefore, the number of holes are related to the concentration of  $NO^0$ , i.e., the number of Si-O bonds. Therefore,  $N_h$  can be expressed as:

$$N_h = NO^0 Av \quad (2-30)$$

where  $Av$  is the Avogadro's number ( $6.023 \times 10^{23}$  /gram mole).

Substituting Eq.(2-29) and (2-30) in Eq. (2-11), the viscosity expression for silicate binary melts is obtained:

$$\eta = 4.9 \times 10^{-9} NO^0 T^{1/2} \exp(E/RT) \text{ poise} \quad (2-31)$$

### 3. CHAPTER CALCULATION AND DISCUSSION

#### 3.1 Pure liquid silica

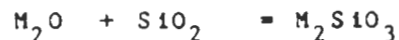
The viscosity of pure liquid silica was calculated using Eq.(2-31). In this case,  $E=519$  Kjoule/mole(19),  $NO^0=1$ , and  $T=2223K$ . The calculated viscosity value is  $3.7 \times 10^5$  (poise), which is in good agreement with the experimental data of  $1.72 \times 10^5$  (poise)(20).

#### 3.2 Binary systems

##### 3.2.1. Alkali metal oxide-silica systems

The viscosity calculation for  $Na_2O-SiO_2$  and  $Li_2O-SiO_2$  systems are shown in this section.

The depolymerization reaction for alkali metal oxide silica system can be written as:



where M is Li, or Na. The free energy change for several systems are given in table 1.

Using equation (2-23) and (2-24), the values of  $NO^0$  was calculated. From the known values of  $NO^0$ , the activation energy using equation (3-1) was obtained.

$$E = E^* / [K(1-NO^0) + 1]^{1/4} \quad (3-1)$$



Table 1. Free energy of reaction

| reaction   | Free energy<br>joule | Ref. |
|--|----------------------|------|
| $\text{Na}_2\text{O} + \text{SiO}_2 = \text{Na}_2\text{SiO}_3$ | $- 234584 + 8.7 T$   | (21) |
| $\text{Li}_2\text{O} + \text{SiO}_2 = \text{Li}_2\text{SiO}_3$ | $- 143792 + 3.7 T$   | (21) |
| $2\text{CaO} + \text{SiO}_2 = \text{Ca}_2\text{SiO}_4$         | $- 118712 - 11.3 T$  | (22) |
| $2\text{MgO} + \text{SiO}_2 = \text{Mg}_2\text{SiO}_4$         | $- 67131 + 4.3 T$    | (21) |
| $2\text{BaO} + \text{SiO}_2 = \text{Ba}_2\text{SiO}_4$         | $- 259578 + 5.0 T$   | (23) |
| $2\text{SrO} + \text{SiO}_2 = \text{Sr}_2\text{SiO}_4$         | $- 213180 + 5.8 T$   | (23) |

It was found that the fourth power gave the better correlation to the experimental data. In the above equation,  $K$  can be solved assuming  $E = BE^*$  when  $NO^0 = 0.5$ , where the value of  $B$  is 0.4838, 0.4889, and 0.4961 for temperature 1623 K, 1673 K and 1723 K, respectively. Thus, the  $K$  values are 34.5, 33, and 31 for 1623 K, 1673 K and 1723 K respectively. The  $K$  value decreases a little bit with increasing the temperature.

The viscosity values calculated using Eq.(2-31), along with the experimental data(24) are shown in Fig.8 to 10 and are also presented in table 2 for temperature 1623, 1673 and 1723. An excellent agreement between calculated and experimental viscosity data is obtained. Fig.11 shows the comparison of calculated values and experimental viscosity data as a function of temperature at constant  $NO^0$ . As expected, at a constant  $NO^0$  values, the viscosity of silicate melts decreases with increasing temperature.

### 3.2.2. Alkaline earth metal oxide-silica systems

The viscosity calculation of  $CaO-SiO_2$ ,  $MgO-SiO_2$ ,  $BaO-SiO_2$  and  $SrO-SiO_2$  system are presented in this section.

The depolymerization reaction for alkali earth system can be considered as:

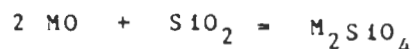


Table 2. Calculated and measured viscosity  
of Alkali metal-silicate binary systems

| Temperature(K)                                | XS <sub>102</sub> | NO <sup>o</sup> | Viscosity (poise) |       |
|---|-------------------|-----------------|-------------------|-------|
|   |                   |                 | Cal.              | Expt. |
| <b>Na<sub>2</sub>O-SiO<sub>2</sub> system</b> |                   |                 |                   |       |
| 1623  | 0.67              | 0.6             | 40.2              | 40.7  |
|   | 0.65              | 0.58            | 31.0              | 32.4  |
| <b>Li<sub>2</sub>O-SiO<sub>2</sub> system</b> |                   |                 |                   |       |
| * K=34.5                                      | 0.6               | 0.5             | 12.3              | 12.3  |
|   | 0.55              | 0.42            | 5.4               | 3.98  |
|   | 0.5               | 0.34            | 2.7               | 1.78  |
|   | 0.45              | 0.25            | 1.3               | 0.63  |
| <b>Na<sub>2</sub>O-SiO<sub>2</sub> system</b> |                   |                 |                   |       |
| 1673  | 0.67              | 0.6             | 27.5              | 28.2  |
|   | 0.65              | 0.58            | 21.5              | 22.9  |
| <b>Li<sub>2</sub>O-SiO<sub>2</sub> system</b> |                   |                 |                   |       |
| * K=33  | 0.6               | 0.5             | 8.6               | 9     |
|   | 0.55              | 0.42            | 3.8               | 3.09  |
|   | 0.5               | 0.34            | 1.8               | 1.4   |
|   | 0.45              | 0.25            | 0.8               | 0.53  |
| <b>Na<sub>2</sub>O-SiO<sub>2</sub> system</b> |                   |                 |                   |       |
| 1723  | 0.67              | 0.6             | 21                | 20.4  |
|   | 0.65              | 0.58            | 16.4              | 16.6  |
| <b>Li<sub>2</sub>O-SiO<sub>2</sub> system</b> |                   |                 |                   |       |
| * K=31  | 0.6               | 0.5             | 6.7               | 7.74  |
|   | 0.55              | 0.42            | 3.0               | 2.51  |
|   | 0.5               | 0.34            | 1.4               | 1.15  |
|   | 0.45              | 0.25            | 0.6               | 0.45  |

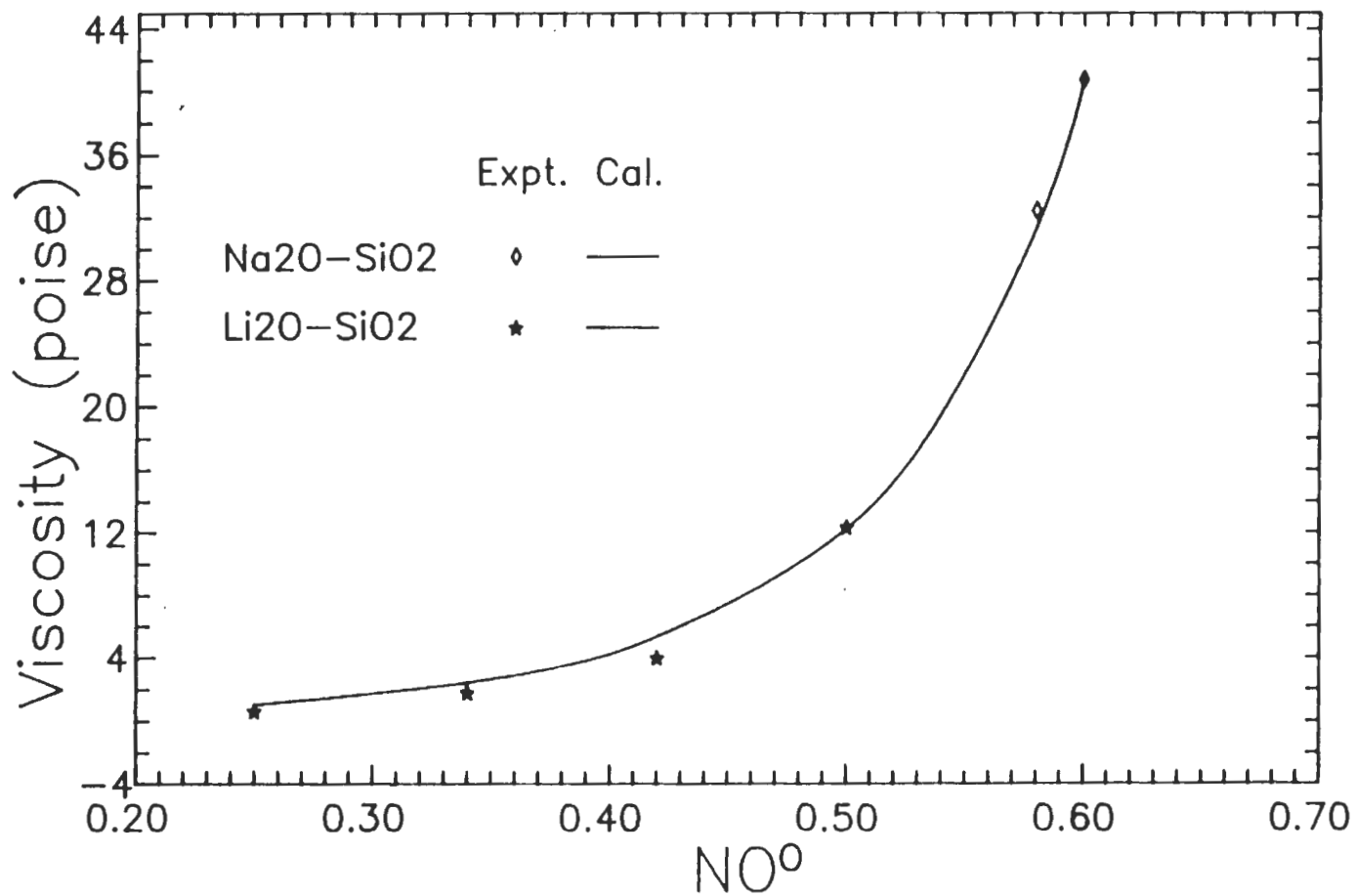


Fig 8. Plot of calculated and measured viscosity of binary systems at 1623 K

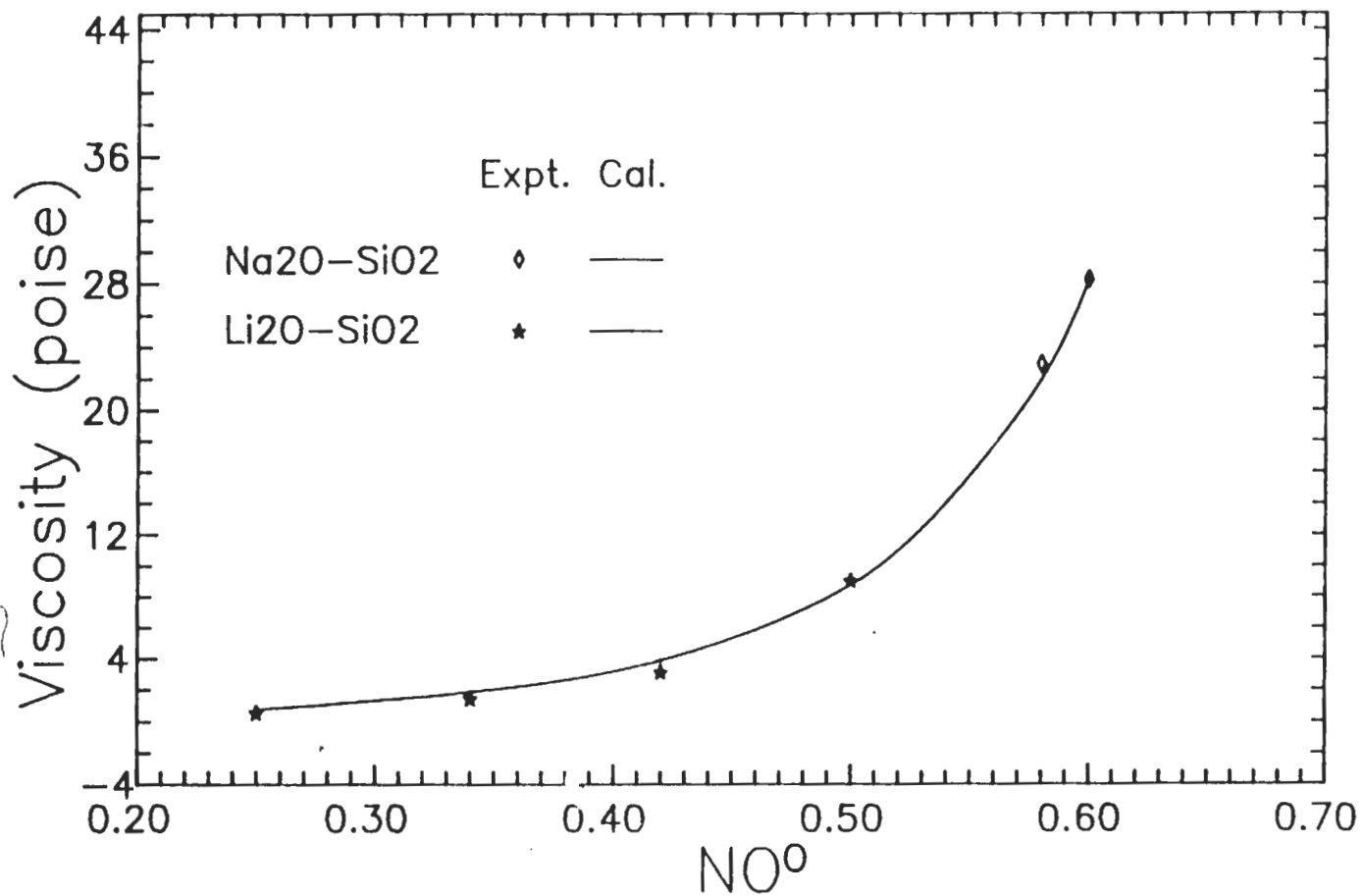


Fig 9. Plot of calculated and measured viscosity of binary systems at 1673 K

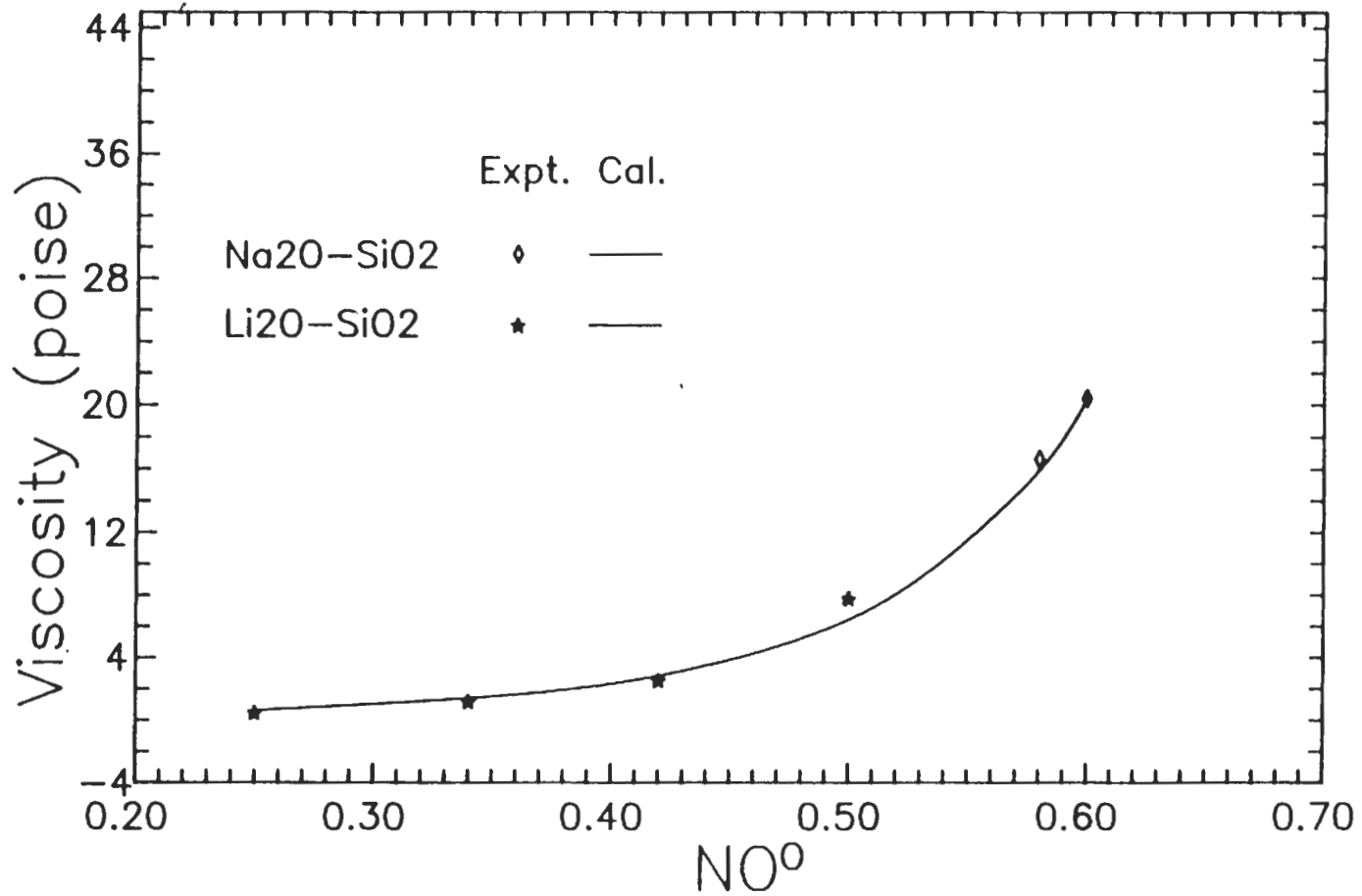


Fig 10 Plot of calculated and measured viscosity of binary systems at 1723 K

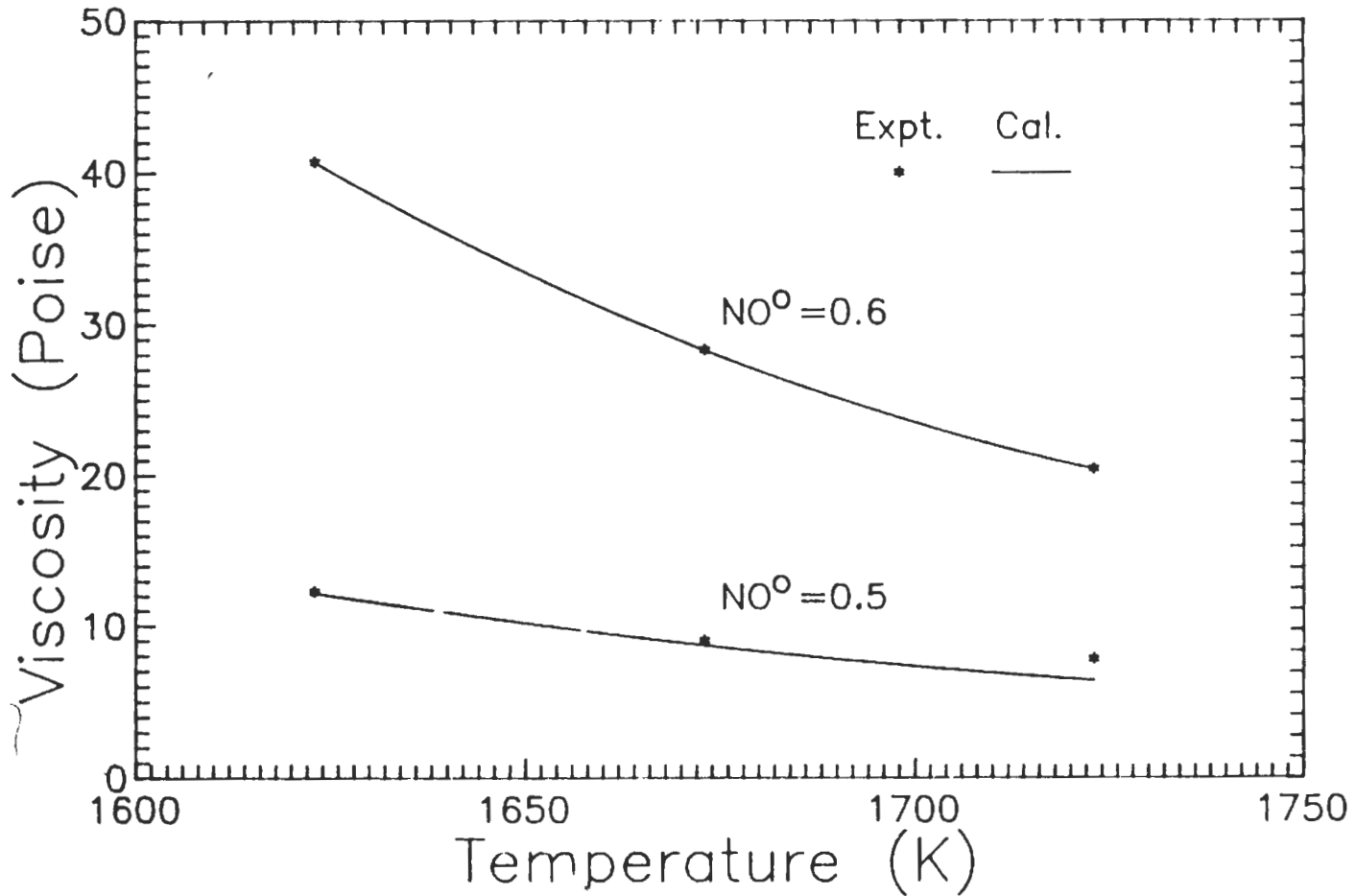


Fig.11. Plot of calculated and measured viscosity of binary system as a function of temperature

where M is equal to Ca, Mg, Sr, and Ba. The free energy change for several systems are given table-1.

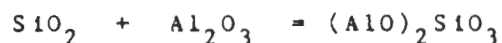
The values of  $NO^{\circ}$  for these binary systems can be obtained from Eq.(2-23) and (2-24). In this case, E as a function of  $NO^{\circ}$  has the following relation:

$$E = E^* / [K(1-NO^{\circ}) + 1]^{1/8} \quad (3-2)$$

The viscosity values for several binary systems calculated using Eq.(2-33) are presented in Fig.12 to 14 and also in table 3 to 5 for temperature 1973 K, 2023 K and 2073 K. A good agreement between the calculated and experimental data(24) is observed.

### 3.2.3. Alumina-silicate system

Alumina, which is an amphoteric oxide, acts as a base in the presence of a strong acid, and acts as an acid in the presence of a strong base(18). For alumina-silicate melts, the depolymerization reaction can be written as(18):



$$\Delta G^{\circ} = -8803 + 3.887T \text{ joule/mole} \quad (24)$$

When N mole of  $SiO_2$  and (1-N) mole of  $Al_2O_3$  mixed to form binary silicate melt, the  $AlO^+$  and  $O^{\circ}$ ,  $O^-$  and  $O^{2-}$  ions coexisted in liquid. The mass balance for oxygen ions can be



Table 3. Calculated and measured viscosity  
of alkali earth metal-silicate system  
( at 1973 K )

| System               | $X_{\text{SiO}_2}$ | $\text{NO}^{\circ}$ | Viscosity (poise) |       |
|----------------------|--------------------|---------------------|-------------------|-------|
|                      |                    |                     | Cal.              | Expt. |
| CaO-SiO <sub>2</sub> | 0.56               | 0.44                | 3.0               | 2.35  |
|                      | 0.52               | 0.36                | 1.8               | 1.5   |
|                      | 0.50               | 0.33                | 1.5               | 1.19  |
|                      | 0.48               | 0.36                | 1.2               | 1.0   |
|                      | 0.46               | 0.29                | 0.9               | 0.9   |
|                      | 0.42               | 0.20                | 0.7               | 0.74  |
| MgO-SiO <sub>2</sub> | 0.557              | 0.46                | 3.5               | 3.6   |
|                      | 0.549              | 0.44                | 3.0               | 2.69  |
|                      | 0.542              | 0.43                | 2.9               | 2.05  |
|                      | 0.5                | 0.37                | 1.8               | 1.49  |
|                      | 0.48               | 0.35                | 1.7               | 1.24  |
| BaO-SiO <sub>2</sub> | 0.6                | 0.5                 | 4.5               | 5.37  |
|                      | 0.58               | 0.47                | 3.7               | 3.31  |
|                      | 0.5                | 0.33                | 1.6               | 1.95  |
| SrO-SiO <sub>2</sub> | 0.59               | 0.48                | 3.9               | 4.79  |
|                      | 0.56               | 0.43                | 2.9               | 2.81  |
|                      | 0.5                | 0.33                | 1.6               | 1.86  |

\* K=230

E=BE\*

at  $\text{NO}^{\circ}=0.5$  B=0.5128

Table 4. Calculated and measured viscosity of  
Alkali earth metal-silicate binary system  
(2023 K)

| System               | $X_{SiO_2}$ | $NO^O$ | Viscosity (poise) |       |
|----------------------|-------------|--------|-------------------|-------|
|                      |             |        | Cal.              | Expt. |
| MgO-SiO <sub>2</sub> | 0.557       | 0.46   | 3.3               | 3.6   |
|                      | 0.549       | 0.44   | 2.9               | 2.7   |
|                      | 0.542       | 0.43   | 2.7               | 2.1   |
|                      | 0.5         | 0.37   | 1.8               | 1.5   |
|                      | 0.48        | 0.35   | 1.7               | 1.2   |
| SrO-SiO <sub>2</sub> | 0.59        | 0.48   | 3.7               | 3.73  |
|                      | 0.56        | 0.43   | 2.7               | 2.14  |
|                      | 0.5         | 0.33   | 1.5               | 1.57  |
| BaO-SiO <sub>2</sub> | 0.6         | 0.5    | 4.3               | 4.57  |
|                      | 0.58        | 0.47   | 3.5               | 2.62  |
|                      | 0.5         | 0.33   | 1.6               | 1.64  |

\* K=190      E=BE\*      at  $NO^O=0.5$       B=0.5235

Table 5. Calculated and measured viscosities of  
Alkali earth metal-silicate binary system  
(2073 K)

| System               | $X_{SiO_2}$ | $NO^{\circ}$ | Cal. | Expt. |
|----------------------|-------------|--------------|------|-------|
| MgO-SiO <sub>2</sub> | 0.557       | 0.46         | 2.85 | 2.83  |
|                      | 0.549       | 0.44         | 2.5  | 2.09  |
|                      | 0.542       | 0.43         | 2.3  | 1.8   |
|                      | 0.5         | 0.37         | 1.6  | 1.18  |
|                      | 0.48        | 0.35         | 1.3  | 1.07  |
| SrO-SiO <sub>2</sub> | 0.59        | 0.48         | 3.2  | 2.95  |
|                      | 0.56        | 0.43         | 2.3  | 1.82  |
|                      | 0.5         | 0.33         | 1.3  | 1.3   |
| BaO-SiO <sub>2</sub> | 0.6         | 0.5          | 3.7  | 3.98  |
|                      | 0.58        | 0.47         | 3.0  | 2.15  |
|                      | 0.5         | 0.34         | 1.4  | 1.5   |

\* K=170

E=BE\*

at  $NO^{\circ}=0.5$

B=0.5319

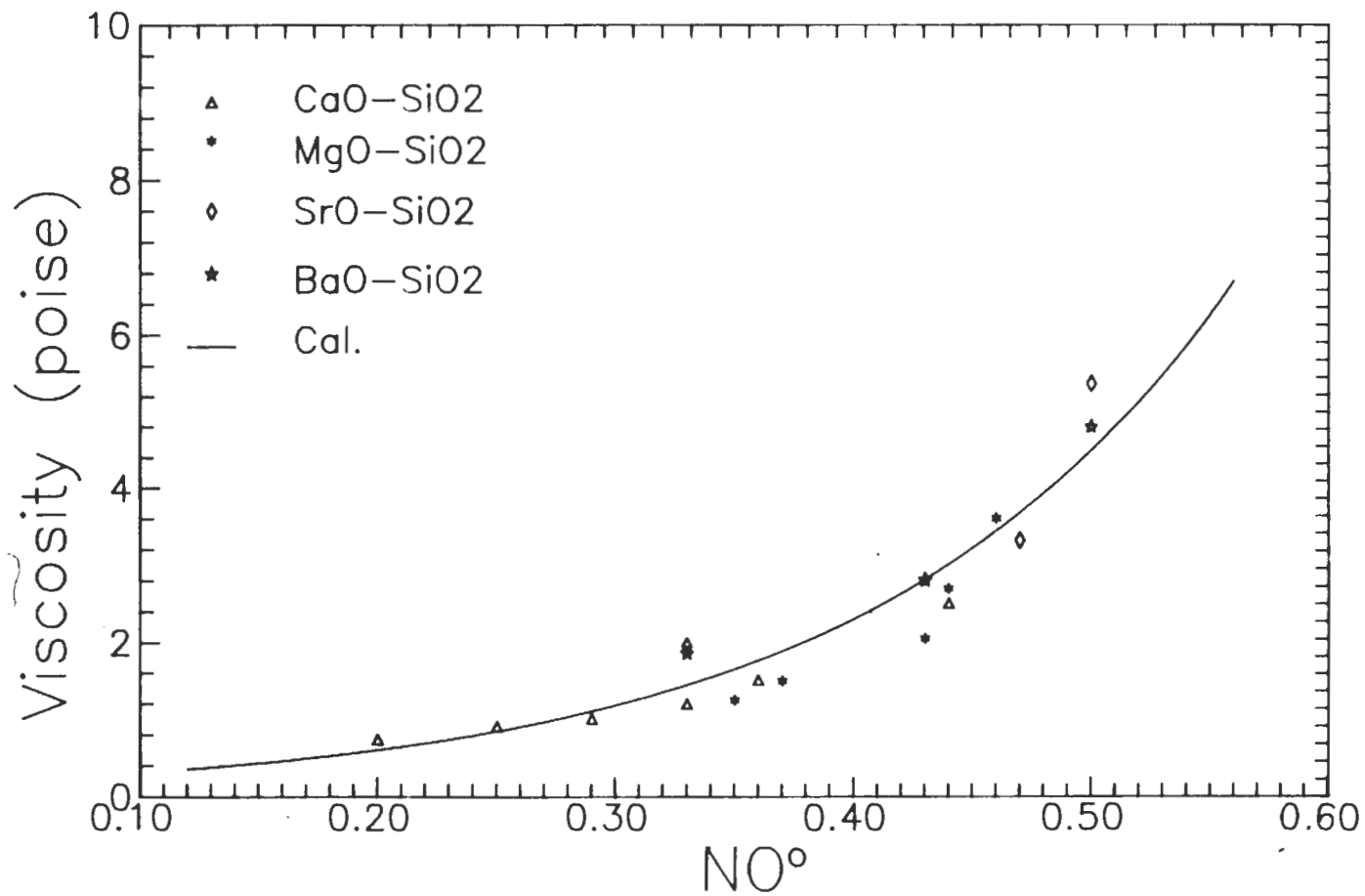


Fig.12. Plot of calculated and measured viscosity of binary system at 1973 K

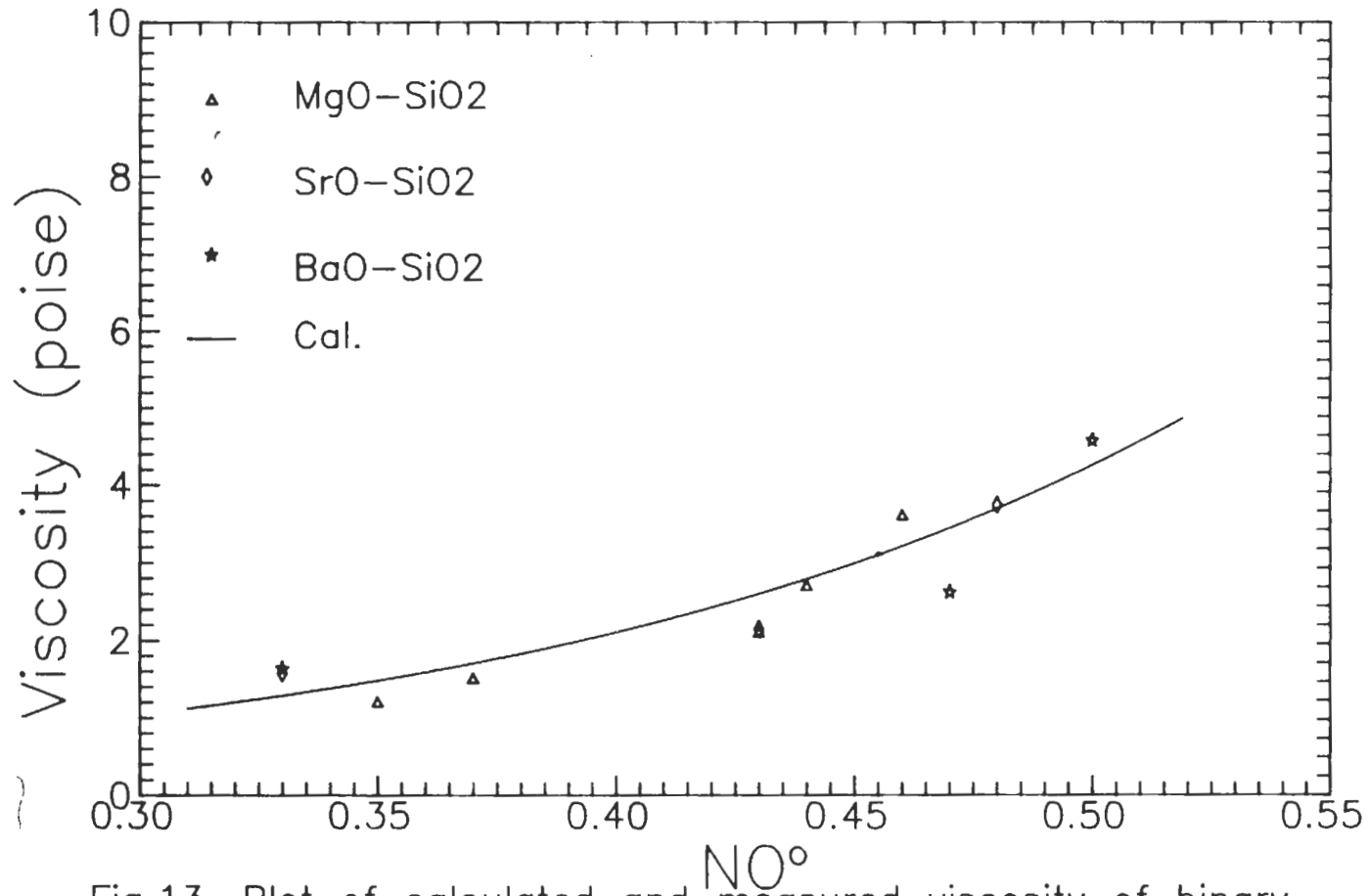


Fig.13. Plot of calculated and measured viscosity of binary system at 2023 K

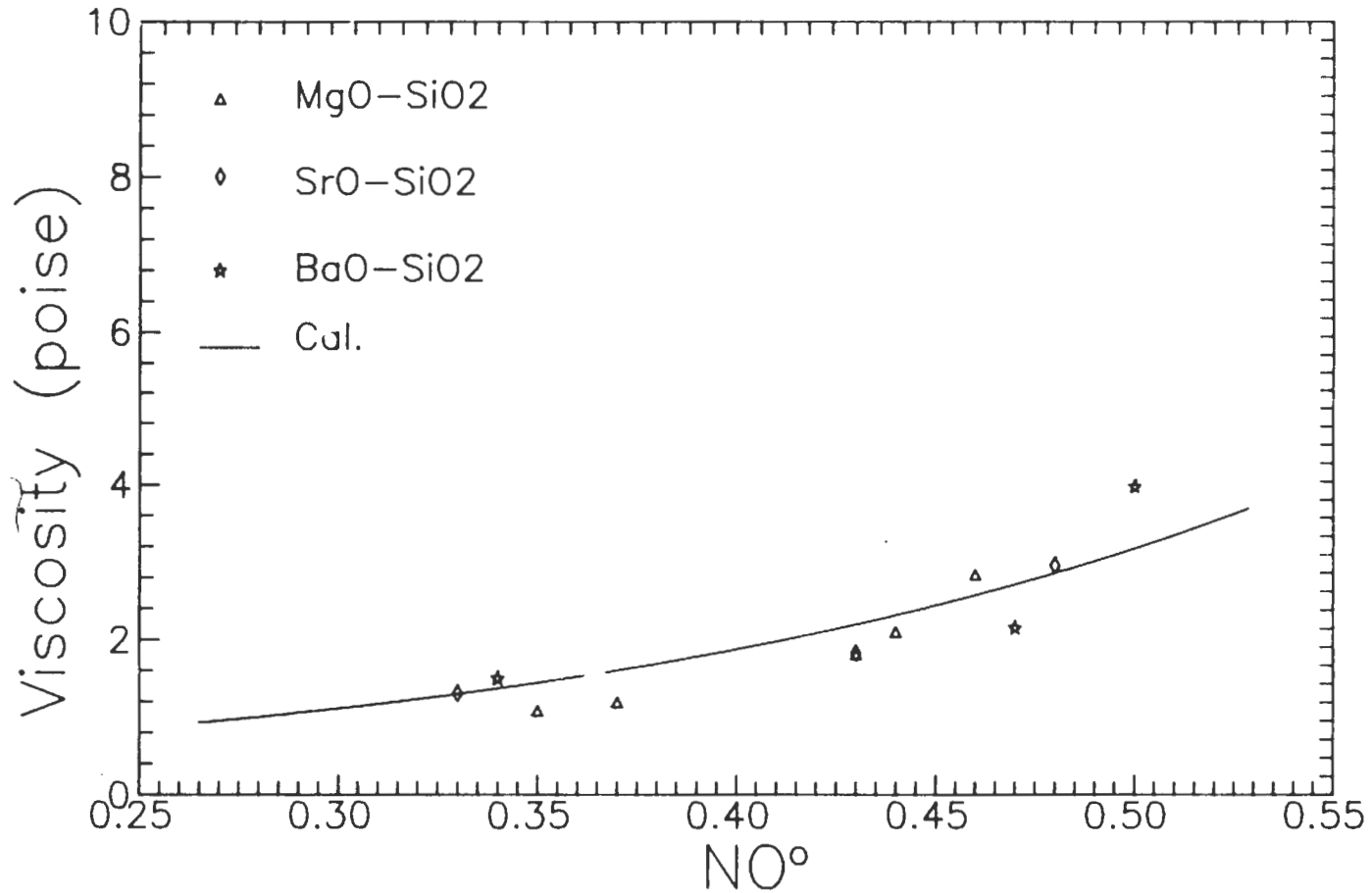


Fig.14. Plot of calculated and measured viscosity of binary system at 2073 K

expressed as(see Fig 7-1):

$$NO^{\circ} = 2N - 1/2 NO^{-} \quad (3-3)$$

$$NO^{2-} = (1-N) - 1/2 NO^{-} \quad (3-4)$$

Thus, the number of  $NO^{\circ}$  can be obtained from Eq.(2-24). Using the same method as mentioned above, the viscosity values were computed using Eq.(2-31). From table 6, it can be found that if M in equation(2-27) equals to 12, it gave the better correlation to the experimental data.

It is interesting to note that there exists a relation between power number M in Eq.(2-27) and the charge of cations Z, as shown in the equation below:

$$M = 4 Z \quad (3-5)$$

Numerical analysis shows that the lower value of M only causes the curve E to be sharper. However, the K value will affect the value of activation energy. The larger the K value, the less the activation energy is needed.

The E increases with increase in Z values, or increases with decrease in K values. This is in agreement with experimental data as shown in Figure 6.

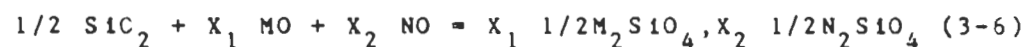
Table 6. Calculated and measured viscosity of  
alumina-silicate system (2223 K)

| $X_{\text{SiO}_2}$ | $\text{NO}^\circ$ | Viscosity                |         |
|--------------------|-------------------|--------------------------|---------|
|                    |                   | Cal.                     | Expt.   |
| 0.8                | 0.79              | 37                       | 39      |
| 0.5                | 0.35              | 3.0                      | 2.0     |
| 0.3                | 0.122             | 0.7                      | 1.0     |
| * K=480            | E=BE*             | at $\text{NO}^\circ=0.5$ | B=0.633 |



### 3.3. Ternary system

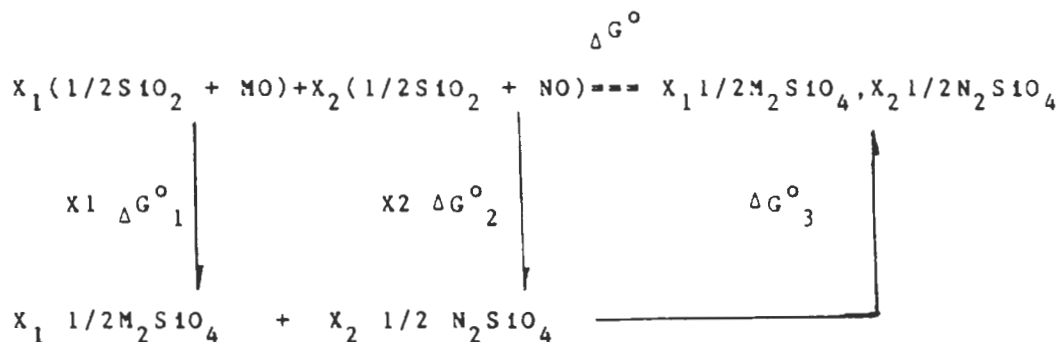
For ternary systems, the melts are considered to be composed of cation ( $M_1^{++}$ ,  $M_2^{++}$ ) and anions ( $SiO_4$ ,  $O^0$ ,  $O^-$  and  $O^{2-}$ ). Each cation can affect the degree of depolymerization of the melts. Let  $N$  mole of  $SiO_2$ ,  $M_1$  mole of  $MO$  and  $M_2$  mole of  $NO$  mix together, and  $M_1 + M_2$  is the total moles of metal oxides, and  $X_1 = M_1/(M_1+M_2)$ ,  $X_2 = M_2/(M_1+M_2)$ . The overall reaction can be written as:



The polymerization reaction can be expressed as:



For the total cyclic process:



Because the free energy  $\Delta G^{\circ}_3$  is very small compared to  $\Delta G^{\circ}_1$  and  $\Delta G^{\circ}_2$ , the free energy change for reaction (3-7) can be simplified as:

$$\Delta G^{\circ} = X_1 \Delta G^{\circ}_1 + X_2 \Delta G^{\circ}_2 \quad (3-8)$$

The mass balance for oxygen ions requires that

$$NO^{\circ} = 2N - 1/2 NO^{-} \quad (3-9)$$

$$NO^{2-} = (M_1 + M_2) - 1/2 NO^{-} \quad (3-10)$$

the total number of anions

$$NO^{\circ} + NO^{-} + NO^{2-} = 2N + M_1 + M_2.$$

The configuration of this pairs is given by

$$(2N + M_1 + M_2)!$$

$$t_{gen} = \frac{-----}{[(M_1 + M_2) - 1/2 NO^{-}]! (NO^{-}/2)! (NO^{-}/2)! [2N - 1/2 NO^{-}]!}$$

Let  $N + M_1 + M_2 = 1$ , then  $M_1 = X_{MO}$ ,  $M_2 = X_{NO}$ , the  $NO^{-}$  values can be deduced by inserting the above conditions into the binary statistical expression given in equation (2-23). The deduced equation is:

$$[1 - \exp(\Delta G^{\circ}/RT)](NO^{-})^2 + [2(X_{MO} + X_{NO}) - 4]NO^{-} + 8[(X_{MO} + X_{NO}) - (X_{MO} + X_{NO})^2] = 0 \quad (3-11)$$

The  $NO^{\circ}$  values can be obtained as:

$$NO^{\circ} = [4 - 4(X_{MO} + X_{NO}) - NO^{-}] / 2[2 - (X_{MO} + X_{NO})] \quad (3-12)$$

The calculated viscosities using equation (3-12), (3-2) and (2-33) for  $MnO-CaO-SiO_2$  and  $MgO-CaO-SiO_2$  system (25-26) are presented in table 7 and 8. As seen from the table, substituting  $MnO$  for  $CaO$  appears to have little effect on viscosities. In this case, the  $M$  in Eq.(2-27) is the same as that in Eq.(3-2), but  $K$  is larger than that in Eq.(3-2). The  $E$  in above ternary systems is less than that in alkaline earth metal-silicate binary system. This may be the interaction effects between  $CaO$  and  $MnO$ , and  $CaO$  and  $MgO$  metal oxides. From known  $NO^{\circ}$  and  $E$  calculated values, respectively, the viscosities calculated for  $CaO-MnO-SiO_2$  system are presented in table 7 and Fig.15. The  $CaO-MgO-SiO_2$  viscosities data are presented in table 8. As seen from the tables and figure, the calculated values agree very well with the experimental data.

The experimental viscosity data for  $CaO-SiO_2-Al_2O_3$  and  $SrO-SiO_2-Al_2O_3$  systems (27-28) are shown in table 10 and 11. The  $NO^{\circ}$  values are computed using Eq.(3-12). The  $M$  in Eq.(2-27) is the same as that in Eq.(3-2), and  $K$  is slightly larger than that in Eq.(3-2). These results are also shown in table 10 and 11. It can be seen from the tables, a good agreement between the calculated and experimental data is observed.

Table 7. Calculated and measured viscosity of  
MnO-CaO-SiO<sub>2</sub> system (1773 K)

| -----             |                  |                   |                         |         |       |
|-------------------|------------------|-------------------|-------------------------|---------|-------|
| Viscosity (poise) |                  |                   |                         |         |       |
| X <sub>MNO</sub>  | X <sub>CaO</sub> | X <sub>SiO2</sub> | NO <sub>o</sub>         | Cal.    | Expt. |
| -----             |                  |                   |                         |         |       |
| 0.3               | 0.3              | 0.4               | 0.15                    | 0.9     | 0.8   |
| 0.4               | 0.2              | 0.4               | 0.155                   | 0.96    | 0.8   |
| 0.5               | 0.1              | 0.4               | 0.16                    | 1.0     | 0.8   |
| 0.1               | 0.4              | 0.5               | 0.34                    | 3.6     | 3.6   |
| 0.2               | 0.3              | 0.5               | 0.34                    | 3.6     | 3.5   |
| -----             |                  |                   |                         |         |       |
| * K=350           |                  | E=BE*             | at NO <sup>o</sup> =0.5 | B=0.524 |       |

Table 8. Calculated and measured viscosity of  
MgO-CaO-SiO<sub>2</sub> system (1723 K)

| -----             |                  |                   |                         |         |       |
|-------------------|------------------|-------------------|-------------------------|---------|-------|
| Viscosity (poise) |                  |                   |                         |         |       |
| X <sub>MgO</sub>  | X <sub>CaO</sub> | X <sub>SiO2</sub> | NO <sup>o</sup>         | Cal.    | Expt. |
| -----             |                  |                   |                         |         |       |
| 0.205             | 0.245            | 0.55              | 0.424                   | 11.8    | 12.2  |
| 0.203             | 0.389            | 0.408             | 0.177                   | 2.06    | 2.89  |
| -----             |                  |                   |                         |         |       |
| * K=350           |                  | E=BE*             | at NO <sup>o</sup> =0.5 | B=0.524 |       |

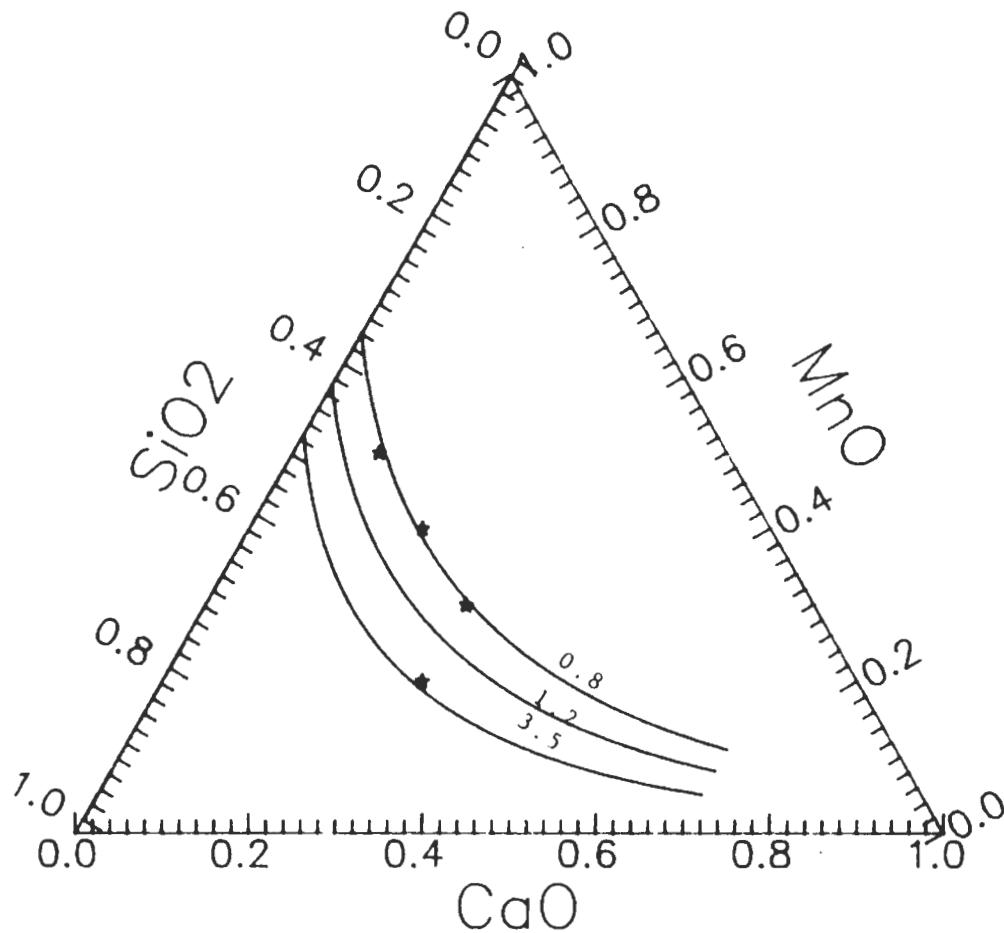


Fig. 15 Plot of calculated and measured viscosity of ternary system at 1773 K

Table 9. Calculated and measured viscosity of  
CaO-SiO<sub>2</sub>-Al<sub>2</sub>O<sub>3</sub> system (1773 K)

| X <sub>CaO</sub> | X <sub>SiO<sub>2</sub></sub> | X <sub>Al<sub>2</sub>O<sub>3</sub></sub> | NO <sup>o</sup>         | Viscosity (poise) |       |
|------------------|------------------------------|--|-------------------------|-------------------|-------|
|                  |                              |  |                         | Cal.              | Expt. |
| 0.54             | 0.4                          | 0.06                                     | 0.16                    | 2.38              | 4.01  |
| 0.48             | 0.45                         | 0.07                                     | 0.25                    | 4.6               | 4.88  |
| 0.43             | 0.5                          | 0.07                                     | 0.35                    | 9.04              | 8.23  |
| 0.38             | 0.56                         | 0.06                                     | 0.43                    | 15.0              | 15.1  |
| 0.33             | 0.61                         | 0.06                                     | 0.52                    | 27.5              | 29.1  |
| * K=250          |                              | E=BE*                                    | at NO <sup>o</sup> =0.5 | B=0.5463          |       |

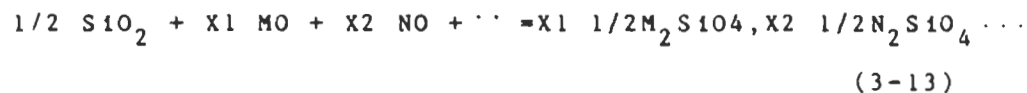
Table 10. Calculated and measured viscosity of  
SrO-SiO<sub>2</sub>-Al<sub>2</sub>O<sub>3</sub> system (1843 K)

| X <sub>SrO</sub> | X <sub>SiO<sub>2</sub></sub> | X <sub>Al<sub>2</sub>O<sub>3</sub></sub> | NO <sup>o</sup>         | Viscosity (poise) |       |
|------------------|------------------------------|--|-------------------------|-------------------|-------|
|                  |                              |  |                         | Cal.              | Expt. |
| 0.3              | 0.65                         | 0.05                                     | 0.57                    | 23.0              | 27    |
| 0.35             | 0.6                          | 0.05                                     | 0.5                     | 14.3              | 15.4  |
| 0.4              | 0.55                         | 0.05                                     | 0.42                    | 8.5               | 9.81  |
| 0.45             | 0.5                          | 0.05                                     | 0.33                    | 4.8               | 5.1   |
| * K=230          |                              | E=BE*                                    | at NO <sup>o</sup> =0.5 | B=0.552           |       |

### 3.4. Multicomponent system

The multicomponent system  $\text{CaO-MgO-Al}_2\text{O}_3\text{-SiO}_2$  is very important slag systems in the BF processes. Therefore, the prediction of viscosities is very important in understanding the metal refining processes.

Let  $N$  mole of  $\text{SiO}_2$  and  $M_1$  mole of  $\text{MO}$ ,  $M_2$  mole of  $\text{NO}$ ,  $M_3$  mole of  $\text{PO}$ , ... form a multicomponent system. The reaction can be considered as:



where  $X_1 = M_1 / (M_1 + M_2 + \dots)$ ,

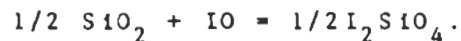
$X_2 = M_2 / (M_1 + M_2 + \dots)$

and  $X_i = M_i / \sum M_i$

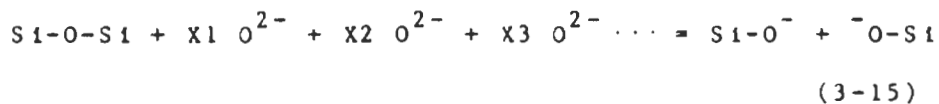
The  $\Delta G^\circ$  for reaction (3-13) is similar to that described in the ternary systems and can be obtained as:

$$\Delta G^\circ = X_1 \Delta G^\circ_1 + X_2 \Delta G^\circ_2 + X_3 \Delta G^\circ_3 + \dots \quad (3-14)$$

$\Delta G^\circ_1$  is the free energy for reaction



The depolymerization reaction is



The  $NO^-$  value is derived as

$$[1 - \exp(\Delta G^0/RT)](NO^-)^2 + [2(M_1 + M_2 + \dots)]NO^- + 8[(M_1 + M_2 + \dots) - (M_1 + M_2 + \dots)^2] = 0 \quad (3-16)$$

The  $NO^0$  value is given as

$$NO^0 = [(4 - M_1 + M_2 + \dots) - NO^-] / 2[2 - (M_1 + M_2 + \dots)] \quad (3-17)$$

For CaO-MgO-SiO<sub>2</sub>-Al<sub>2</sub>O<sub>3</sub> system, the composition is given in table 11, and the  $NO^0$  values are calculated by Eq.(3-17). The E form for this system is the same as that for CaO-SiO<sub>2</sub>-Al<sub>2</sub>O<sub>3</sub> system. The calculated viscosity values are shown in table 11. As seen from the table, the calculated values are in good agreement with the experimental data.

In general, it can be concluded that this model predictions are in better agreement with the experimental data when  $NO^0$  values are higher than 0.2 ( $NO^0 > 0.2$ ). When  $NO^0 < 0.2$ , it can be considered as a complete depolymerization, i.e., less Si-O bonds exists. In this range, the correlation of E values should include the energy needed to form a hole to get a better agreement with the experimental data. Similarly, as the temperature increases, the internal energy also increases. This was observed in the present case. The K decreases with the increase in the temperature (i.e. E increased)



Table 11. Calculated and measured viscosity of  
CaO-MgO-SiO<sub>2</sub>-Al<sub>2</sub>O<sub>3</sub> system (1773 K)

| X <sub>CaO</sub> | X <sub>MgO</sub> | X <sub>SiO2</sub> | X <sub>Al2O3</sub> | NO <sup>o</sup> | Viscosity(poise) |      |
|------------------|------------------|-------------------|--------------------|-----------------|------------------|------|
|                  |                  |                   |                    |                 | Cal.             | Expt |
| 0.475            | 0.075            | 0.395             | 0.058              | 0.15            | 2.2              | 3.09 |
| 0.363            | 0.144            | 0.436             | 0.057              | 0.234           | 4.39             | 4.3  |
| 0.372            | 0.074            | 0.496             | 0.058              | 0.335           | 8.21             | 8.57 |

\* K=250                      E=BE\*                      at NO<sup>o</sup>=0.5                      B=0.5463                      °

## 4. CHAPTER

### 4.1. INTRODUCTION

Potlining is generated in the electrolytic process of reducing alumina to make aluminum metal using molten fluoride electrolytes. Spent potlining (SPL), obtained at the end of the pot's life (about 3 to 5 years), contains a small amount of cyanide and fluorides and thus presents an environmental problem. In addition, SPL also contains significant quantities of useable C and Na and Al fluorides(29). For these reasons, many alternative methods have been investigated that address the recovery of valuable chemicals and energy resources(30-31) and the disposal and/or destruction of SPL(32-33). These methods were reviewed in detail during an Aluminum Association workshop(34). The recycling/disposal method, (SPL would be destroyed or utilized by another industry) is considered the most feasible solution to disposal problems to that of recovery methods(29). The use of spent potlining as a substitute for fluorspar( $\text{CaF}_2$ ) as a fluxing agent in molten pig iron and steel making was reported(32-33). In these studies, the SPL was found to be a satisfactory substitute and no significant adverse effects were noted in the final metal produced. However, no data are available on viscosity of SPL flux at present.

In the present study, The experimentally measured data on viscosity of industrial spent potlining were reported as a function of temperature and with oxide additions to the SPL.

#### 4.2. EXPERIMENTS

##### Materials:

The chemical composition of the industrial SPL used in this study is shown in Table 12. Calcium oxide( $\text{CaO}$ ) and silica( $\text{SiO}_2$ ) powders used were of commercial grade(99% pure).

##### Procedure:

Viscosities were measured using a Brookfield viscometer (RVT DV-II). The viscometer rotates a spindle, which is indicated by deflection of a spring, and is converted to a viscosity value by means of a calibration factor. The RVT model is capable of measuring approximately 0.1 to 200 poise by varying the rotating speed from 100 to 0.5 rpm. The experimental set-up used is shown in Figure 16. A graphite crucible filled with the prefused SPL with or without oxide was heated in a SiC heating element furnace. Once the preset temperature was attained, the graphite spindle was lowered and centered from the bottom of the crucible. Experiments were carried out under the inert gas atmosphere by passing argon gas into the measuring chamber throughout the experiment.

Table 12. The chemical composition of SPL (wt %)

| $\text{Al}_2\text{O}_3$ | C    | F    | CaO | $\text{SiO}_2$ | $\text{Na}_2\text{O}$ | other |
|-------------------------|------|------|-----|----------------|-----------------------|-------|
| 14.4                    | 34.8 | 12.5 | 3.0 | 5.3            | 20                    | 10    |

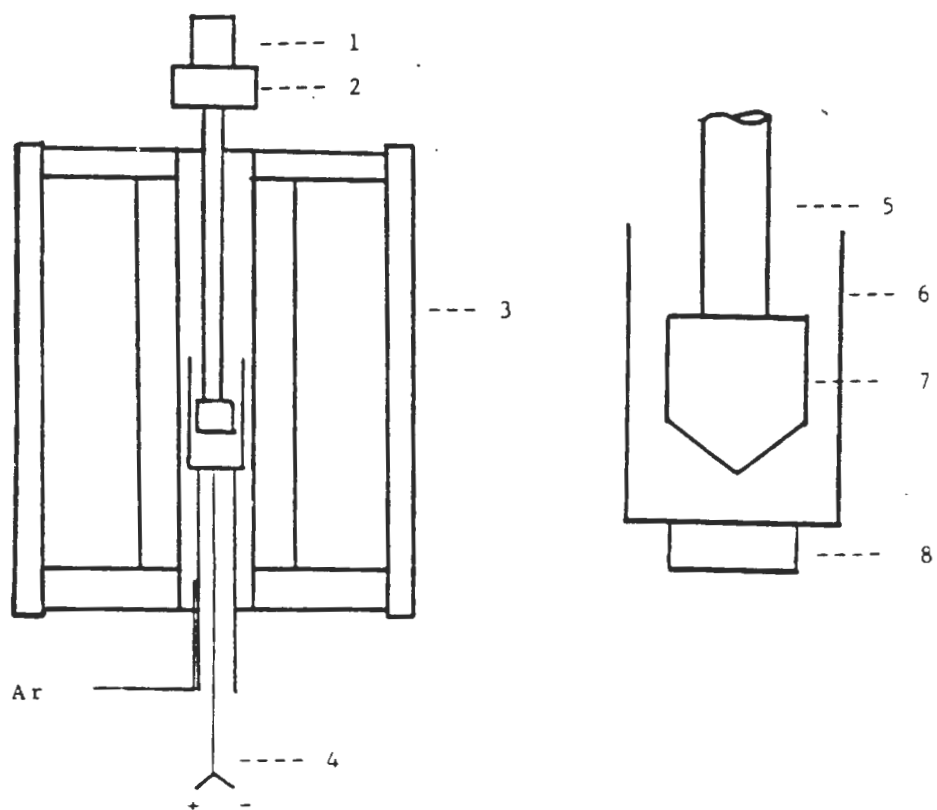


Fig. 16 Experimental Set-up

1 - Motor  
 2 - Torque measuring head  
 3 - Furnace  
 4 - Thermocouple

5 - Driven shaft  
 6 - Crucible  
 7 - Bob  
 8 - Support

Viscosity values were recorded after thermal equilibrium is established. Viscosity measurements were made in a decreasing temperature mode of approximately 50°C intervals after the SPL flux sample had been slowly heated to the desired temperature, typically about 1473 to 1813 K. The experiments were carried out using SPL and also with the addition of SiO<sub>2</sub> and CaO as a function of temperature.

#### 4.3. RESULTS AND DISCUSSION

The experimental data are presented in Figure 17. As seen from the figure, the viscosities of SPL can be significantly be decreased with the addition of metal oxides and an increase in temperature. For example, the viscosity of SPL decreased from 188 to 57.6 poise as the temperature increased from 1623 to 1813 K respectively. As expected, the measured viscosities in the case of CaO addition to SPL melts are found to be much lower than the SPL alone or with the addition of SiO<sub>2</sub> to SPL melts. For example, the viscosities of SPL decreased with the addition of 20 wt% CaO, to 0.132 poise at 1560 K and with the addition of 20 wt% SiO<sub>2</sub>, to 23 poise at 1573 K. As indicated in the review paper by Mills(35), inconsistencies exist in the published viscosity data for pure CaF<sub>2</sub> melt. The reported data on pure CaF<sub>2</sub> at 1773 K is in the range of 0.06 to 0.31 poise and is shown in Figure 17. The addition of 20 wt% CaO to the SPL decreases the viscosity of SPL to a value below

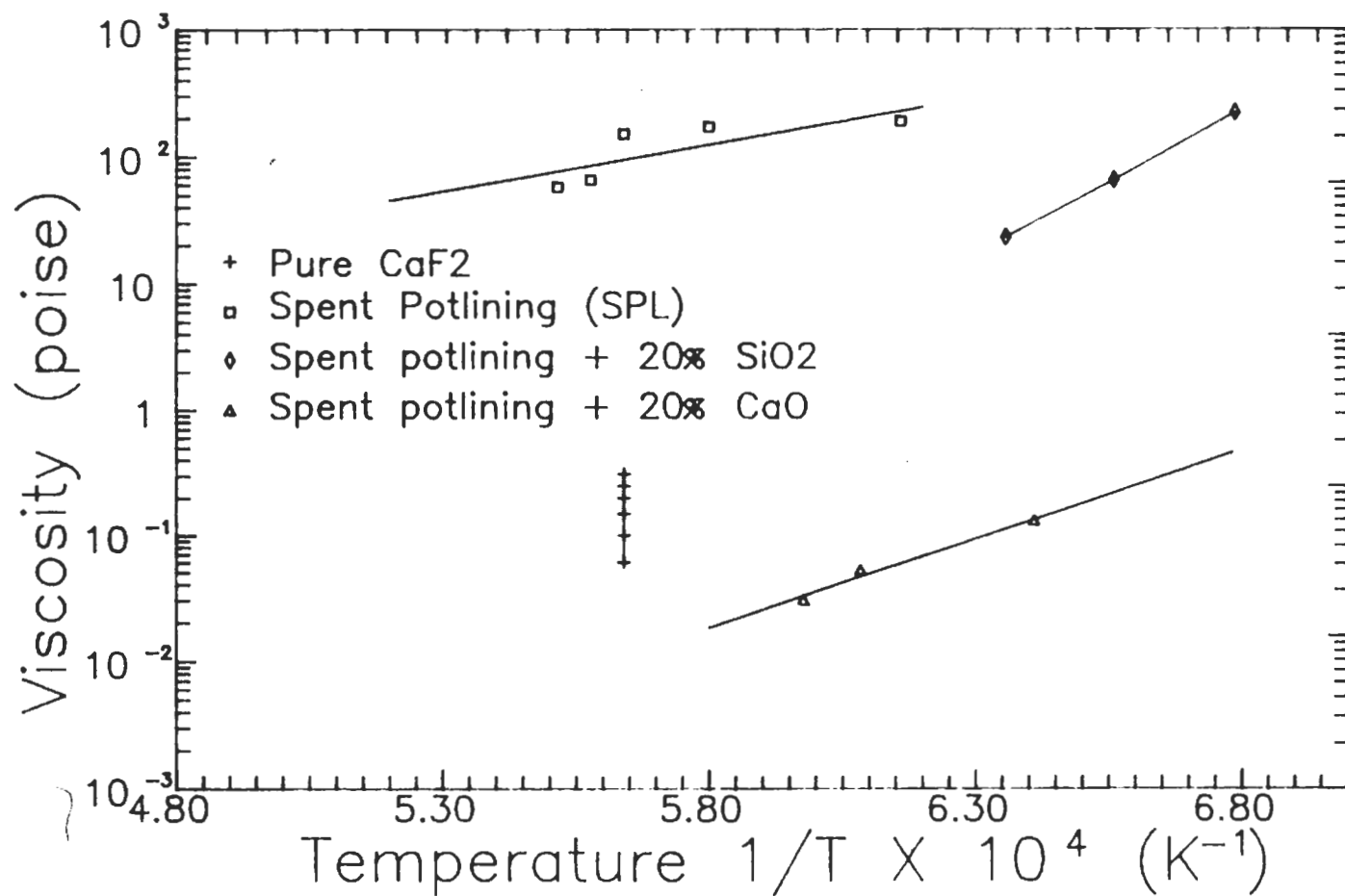


Fig. 17 The measured viscosities data of SPL

that of liquid  $\text{CaF}_2$ . These data also indicate that viscosities equivalent to  $\text{CaF}_2$  can be obtained with a small amount of metal oxide addition to the SPL. Thus, further studies are required to completely assess the viscosity of SPL with varying metal oxide additions to be considered as a substitute for  $\text{CaF}_2$ , under the conditions of hot metal treatment.

The viscosity-temperature relation is typically expressed in the form of Arrhenius equation where the Ln of viscosity in a linear function of the reciprocal absolute temperature. This is true for many liquids. However, some liquids, as shown in Figure 17 for SPL, exhibit a non-linearity on a Ln vs.  $1/T$  plot.

A linear regression equation, Arrhenius type ( $\eta = a \exp(E/RT)$ ), was used to describe the present experimental data. These expressions are given below:

$$\text{For SPL:} \quad \eta = 7.1 \times 10^{-3} \exp(16844/T) \quad (4-1)$$

with a correlation coefficient of 0.8.

$$\text{For SPL+20 wt\% CaO} \quad \eta = 5.2 \times 10^{-11} \exp(33863/T) \quad (4-2)$$

with a correlation coefficient of 0.99.



For SPL+20 wt% SiO<sub>2</sub>:  $\eta = 1.56 \times 10^{-13} \exp(51350/T)$  (4-3)

with a correlation coefficient of 0.99.

As seen from the Table 12, a considerable amount of solids exit in the industrial SPL. Further experimental measurements are needed to understand the effect of the presence of a solid phase like carbon in the melt on viscosity of SPL. Because non homogeneous nature, multicomponents and solid carbon exists, the above model can not be applied to correlate viscosity of the SPL data at this time. Further work in this application is suggested.

## 5. CHAPTER

## CONCLUSION

A significant advance in evaluation of the viscosity model has been achieved as a result of the application of the structural theory to these systems. The major advantage of this approach over any other is the provision of a direct link between ionic constitution and viscosity of slags.

A correlation was made using the hole theory and the structure of melts to express the temperature and  $NO^{\circ}$  dependence of viscosity. The correlation is given by:

$$\eta = 4.9 \times 10^{-9} NO^{\circ} T^{1/2} \exp(E/RT) \quad \text{poise}$$

This equation was successfully applied to predict the viscosity of several binary, ternary and multicomponent metal oxide-silicate systems.

The viscosities of industrial spent potlining (SPL) were measured as a function of temperature and with the addition of 20 wt% CaO or SiO<sub>2</sub> to the SPL. The results show that the viscosity of SPL decreases with increasing temperature and also decreases with the addition of 20 wt% CaO or 20 wt% SiO<sub>2</sub> to SPL at a given temperature.

## 6. CHAPTER

## REFERENCE

1. W.L.McCauley and D.Apelian: 'Temperature Dependence of the Viscosity of Liquids', Second international symposium on metallurgical slags and fluxes, H.A.Fine and D.R.Gaskell, eds. TMS-AIME, lake tahoe, NV, 1984, pp.925.
2. R.Altan, G.stavropoulos, K.Parameswaran and R.P.Goel: 'Viscosity Measurements of Industrial Lead Blast Furnace Slags', Physical chemistry of extractive metallurgy', TMS-AIME, New York, 1985, pp.97.
3. H.F ring and M.S.Jhon: 'Significant liquid structures', John Wiley and Sons, New York, 1969.
4. K.Glasstone, K.J.Laidler, and H.Eyring, The theory of Rate Processes, McGraw-Hill Book Company, New York, 1941.
5. D.Turnbull and M.H.Cohen, J.Chem.phys., Vol.34, pp.120, 1961.
6. G.Adam and J.H.Gibbs, J.Chem.Phys., vol.43, pp.139, 1965.
7. E.T.Turkdogan and P.M.Bills, Am.Ceram.Soc.Bull., 1960,vol.39,pp.682.
8. R.Higgins and T.J.B.jones, Bull.Inst.Min.Netall., 1963,vol.72,pp.825.
9. J.M.Toguri et al, Can.Metall.Q., 1964, vol.3,pp.197.
- 10.Y.Bottinga and D.F.Weill, Am.J.Sci., 1972,vol.272,pp.438.
- 11.G.URBAIN. The J. of Materials Education, V.7, N.6, 1985, pp.1007-1078

12. Bokris and Reddy: 'Modern electrochemistry' pp578, New York, 1970.
13. R. Furth, Proc. Cambridge Phil. Soc., 1941, pp.252-281
14. J. Gotz and C.R. Masson, J. Chem. Soc. Section A, 1970, pp.2683.
15. Yoshio Waseda, Can. Metall. Quar., Vol.20, pp.57-67, 1981.
16. E.A. Guggenheim: Mixtures, Oxford Press, (1952).
17. Y. Kaneko and Y. Suginozawa, Japan Inst. Metals, Vol.12, pp.285-289, 1987.
18. F.D. Richardson: 'Physical chemistry of melts in Metallurgy', pp.95, 1974.
19. R. Bruckner, Glastechn. Ber., 1964, vol.37, pp.413.
20. R. Rossin, L. Bersan and G. Urbain, Rev. Int. Hautes Temp. Refract., 1964, vol.1, pp.159.
21. D.R. Stull and H. Prophet: 'JANAF Thermochemical tables,' NSRDS-NBS37. U.S. Dept. Commer., Washington, D.C., 1971.
22. I. Barin, O. Knacke, and O. Kubaschewski, 'Thermochemical Properties of Inorganic Substances, Supplement.' Springer-Verlag, Berlin and New York, 1977.
23. I. Barin and O. Knacke 'Thermochemical properties of Inorganic Substances.' Springer-Verlag, Berlin and New York, 1973; Metall. Trans., Vol.5, pp. 1769, 1974.
24. J.O.M. Bockris and D.C. Lowe: Proc. R. Soc., Vol.226A, pp.423, 1954
25. L. Segers, A. Fontana and R. Winana, Trans. Inst. Min. Metall., Section C, 1979, vol.88, pp.53.

26. Y. Bottinga and D. F. Weill, *American Journal of Science*,  
vol. 272, pp. 438-475, 1972.
27. K. Mizoguchi, M. Yamane and Y. Kaneko, *J. Japan Inst. Metals*,  
Vol. 48, No. 12, 1984, pp. 1179-1186.
28. J. S. Machin and T. B. Yee, *J. of the American Ceramic Soc.*,  
vol. 31, pp. 200-204, 1948.
29. L. C. Blayden and S. G. Epstein, *Spent Potlining Symposium*,  
*J. of Metals* pp. 22-23, 1984.
30. A. F. Bopp and J. M. Brupbacher, *Light Metals*, AIME,  
pp. 1081-1099, 1986.
31. R. C. Dickie, *J. of Metals*, pp. 28-29, 1984.
32. V. R. Spironello and R. H. Nafziger, *USBMM*, RI 8530, pp. 14,  
1981.
33. D. R. Augood, R. J. Schlager and P. C. Belding, *Light Metals*,  
AIME, pp. 1091-1103, 1983.
34. *Proceedings of the Workshop on Storage, Disposal, and  
Recovery of Spent Potlining*, The Aluminum Association,  
1981.
35. K. C. Mills and B. J. Keene, *Intern. Metals. Rev.* No. 1,  
pp. 21-69, 1981.